Project Number: GSI 0901

The Phase Transitions of 4'-n-pentyl-4-cyanobiphenyl + C_{60} Colloidal Composites

A Major Qualifying Project Report

submitted to the Faculty

of the

WORCESTER POLYTECHNIC INSTITUTE

in partial fulfillment of the

Degree of Bachelor of Science in Physics

By

Steven Ellis

Date: April 28th, 2010

Approved:

_____

Professor Germano S. Iannacchione, Physics advisor

Contents

List of Figures

Acknowledgments

I would first like to thank my advisor, Professor Germano Iannacchione, for his support and his insight into the nature of liquid crystals and order-disorder phenomena. I would like to thank Raj Basu for taking the time to teach the dielectric spectroscopy technique. I would like to thank Nihar Pradhan for showing me how to operate the MDSC machine, how to work with TA Analysis, and how to work with Origin. I would like to give a special thanks to Krishna Sigdel for teaching me proper lab procedures, how to properly use a polarized light microscope, and giving me the overall guidance necessary to complete this project. Lastly, I would also like to thank my family for always believing in me, urging me to stay in school, and helping me achieve the goals I set for myself. I appreciate what you all have done for me; it means a lot and will never be forgotten, thank you.

Abstract

This project is designed to experimentally determine how the nematic-isotropic phase transitions of numerous colloidal composites consisting of the anisotropic liquid crystal 5CB and symmetric nanoparticle C_{60} change as C_{60} mass concentration increases. Composites were placed in a MDSC and were heated and cooled at different frequencies and temperature ramp rates. Using this thermo-analytical technique comparisons of different concentration's reversible and nonreversible heat capacitance signals were analyzed which yielded values for the isotropic to nematic phase transition temperature, enthalpy during the transition, and the coexistence region of both phases during the transition. The analysis showed some unexpected fluctuating results. Images of the different concentrations were taken using a polarized light microscope, the images showed isolated domains of C_{60} and 5CB. To test whether the unexpected results were due to these domains and steric in nature a mechanically quenched macroscopic model of the different composite concentrations was constructed and tested. This steric modeling confirmed that the local domains were due to the unique geometries of the 5CB and C_{60} molecular structure and that steric volume packing may account for the unexpected thermal results.

1. Introduction

1.1 Thermodynamics Review

Thermodynamics is the study of energy and how energy is transformed. The application of thermodynamics begins with defining a thermodynamic system.[1] Once a thermodynamic system is identified the thermodynamic states of the system components can be analyzed. A thermodynamic state is a specific set of well define values for the various thermodynamic properties. Thermodynamic equilibrium is where the thermodynamic states stay the same meaning there is no change in the system's thermodynamic properties. There are only four thermodynamic properties which can be directly measured they are temperature, volume, pressure, and mass. These four properties are directly related to the non-measurable thermodynamic such as entropy, internal energy, enthalpy, Gibbs free energy, heat capacitance by thermodynamic functions also known as Maxwell Relations.[1] For more information on these relations see Thermal and Statistical Physics by Gould and Tobochnik. Temperature is basically a measure of the amount of motion the atoms possess in a given system, the more motion the higher the temperature. Enthalpy is defined as the system's internal energy added to the product of the system's pressure and volume. Heat capacity is the ratio of heat absorbed by at material to the temperature change. The latent heat is the heat absorbed or released as the result of a phase transition.[1] This project will focus on properties such as temperature, heat capacitance, enthalpy, and latent heat.

1.2 Phases

Phases are defined as thermodynamic states of matter, differing in degree and kind of order .[2] The classical phases of matter are solid, liquid, and gaseous. For example water has three phases solid (ice), liquid, and gas (steam, vapor). There are phases and phase transitions other than the classical ones such as plasmas, gels, and liquid crystals. Liquid crystals show an intermediate phase between the

conventional solid and liquid phases. The materials that exhibit these intermediate phases are commonly referred to as mesogens and the phases are known as mesophases.[3]

1.3 Phase Transitions

A phase transition is defined as the transformation of a thermodynamic system from one phase to another. Classic phase transitions include solid to liquid (melting), liquid to gaseous (boiling), and the reverse gaseous to liquid (condensation), and liquid to solid (freezing). Phase transitions can be first ordered or second ordered. Ehrenfest first defined a first order phase transition as a discontinuity in the derivative of some thermodynamic variable (enthalpy, heat capacitance, ….) with respect to the system's free energy and a second order phase transition as a discontinuity in the second derivative. Ehrenfest's model is flawed in some systems in systems. Modern thermodynamics says a first order phase transition is one in which latent heat is present while in a second order phase transition there is no latent heat.[4] This project will deal with first order phase transitions.

1.4 The Liquid Crystal Mesophase

The first scientific observation of a liquid crystal was in the 1850s by Virchow, Mettenheimer and Valentin; while studying a nerve fiber, they found that when placed in water the nerve fiber turned fluid like and exhibited some strange behavior when looked at with polarized light, unbeknownst to them the substance was liquid crystalline.[5] The next observation in the history of liquid crystals was by the Austrian botanist/chemist Friedrich Reinitzer in 1888 at the University of Plant Physiology which was a subset of the University of Prague. Reinitzer was extracting cholesterol from carrots trying to determine to determine the correct molecular weight and formula of cholesteryl benzoate.[6,7] To determine the molecular weight and formula, Reinitzer had to find the exact melting point of cholesteryl benzoate. As he performed the experiment to find the melting point Reinitzer noticed that cholesteryl benzoate seemed to have two melting points, one at 145.5°C and the other at 178.5°C degrees. The first melting point made the cholesterol appear as a cloudy liquid and at the next melting point the liquid

became clear and transparent.[8] The transition also appeared reversible. Reinitzer first took this strange behavior to be impurities in his sample but after repeated attempts and further purification he sent a sample to German physicist Otto Lehmann for analysis. Lehmann put the cloudy sample under a polarized microscope and observed the molecules to be in a crystalline structure while still flowing like a conventional liquid. He dubbed the newly discovered phase of matter a liquid crystal. Approximately 5% of all organic compounds exhibit some liquid crystalline behavior.[9]

1.5 Liquid Crystal Phases

Liquid crystals have the unique reversible ability to have many different phases between the classic solid and liquid phase. A liquid crystal phase can be determined based on the order of its molecular structure or order parameter S, which is defined as,

$$S = \left(\frac{1}{2}\right)\langle 3cos^2\phi - 1\rangle = P_2\langle cos\phi\rangle$$

where ϕ is an angle measured along a dimensionless unit vector $\hat{\boldsymbol{n}}$ called the director which is used to represent the preferred direction that the molecules fluctuate around and the <> brackets represent a thermal averaging. The order parameter is also equal to an average of the second Legendre polynomial.[10]

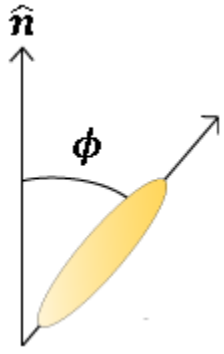

Figure 1 Illustration of the Director[11]

The closer to one S is the more ordered the liquid crystal is and the closer to zero the more disordered the liquid crystal is. If the order parameter is one then the material is solid crystal ($S = 1$ and

$\langle \cos^2 \phi \rangle = 1$) and if the order parameter is zero then the material is an isotropic liquid ($S = 0$ and $\langle \cos^2 \phi \rangle = \frac{1}{3}$).[3] Typically as temperature rises the order decreases and vice versa. All liquid crystals phase transitions are a function of temperature. A thermotropic liquid crystal is organic and has phase transitions dependent upon temperature alone. A lyotropic liquid crystal is also organic but is a mixture of certain molecules and solvents and has phase transitions dependent upon temperature and the ratio of the molecules to the solvents. This project will focus on a thermotropic liquid crystal colloidal composite. A summary of the relationship between order, temperature, and the liquid crystal phase can be seen below in Figure 2.

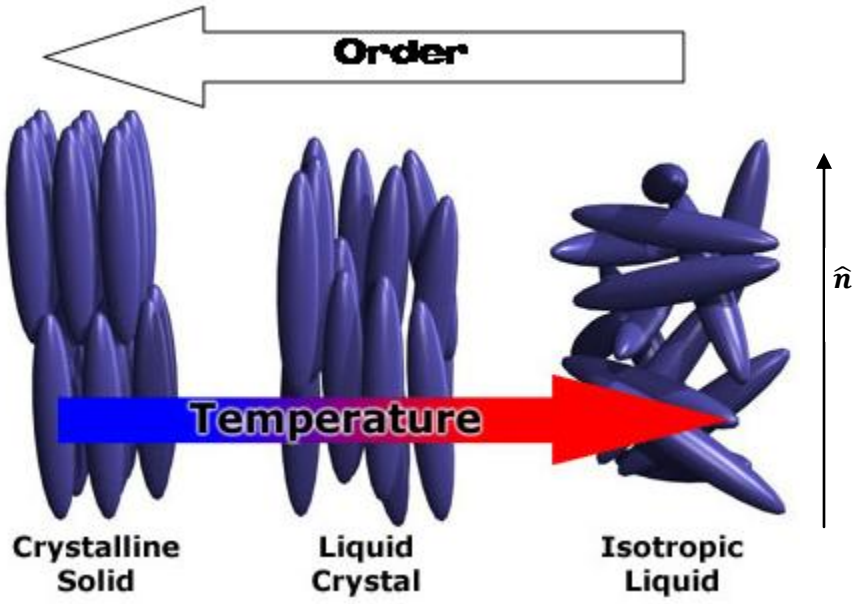

Figure 2 Liquid crystal Temperature/Order[12]

The lowest ordered phase of a liquid crystal, where the order parameter is zero, is at higher temperatures in comparison to the other phase temperatures (above the Critical Temperature T_c), the bulk liquid crystal structure will become an isotropic liquid while the molecules are anisotropic. In an isotropic liquid the molecules are free to move wherever they like and their positional order and orientation is totally random, a director doesn't exist. As an isotropic liquid the molecules have the same properties in all directions.[2] The liquid crystal in the isotropic phase will have no long range order but

will possess some short range order caused by intermolecular interactions. The short range order can be viewed as remnants of the nematic order and the concept is analogous to boiling water, at the critical temperature water will begin to boil but won't all boil at once and there will be remnants of the liquid phase.[3] DeGennes introduced a Laude type phase transition theory based on a short range order parameter to describe the isotropic phase transition.[3] An example of the molecules in an isotropic liquid crystal can be seen in Figure 3.

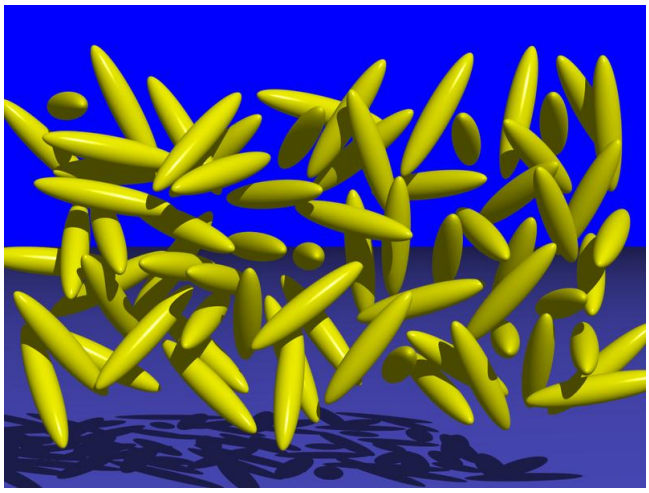

Figure 3 Isotropic Liquid[13]

The Nematic phase is the most simple liquid crystal phase; it is very fluid like and is the phase closest to an isotropic liquid while still exhibiting anisotropic tendencies. The word nematic was derived from the Greek word νημα which translates to thread because of the appearance of thread like defects in the surface of the liquid crystal when viewed through a polarizing microscope.[10] In the nematic phase liquid crystal molecules have no positional order but possess some degree of long range orientational order and align themselves in some direction that is defined as the director.[2,7] Maier and Saupe introduced a simple way to describe liquid crystals in order to explain the phase transition and the behavior of the long range order parameter when approaching the critical phase transition temperature T_c.[14] The theory treats the liquid crystal molecules as rigid rods and they are correlated with one another by Coulomb interactions.[3] Figure 4 represents the molecules in the nematic phase.

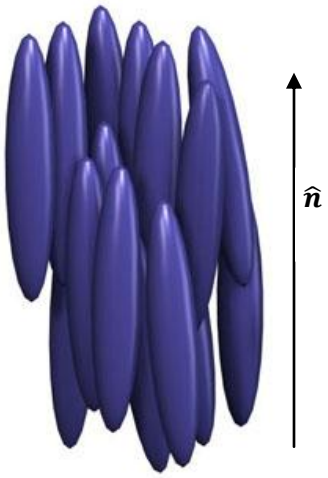

Figure 4 Nematic Liquid Crystal[12]

Molecules in the nematic phase tent to be centrosymmetric meaning they are identical along $+\hat{n}$ and $-\hat{n}$. The individual molecules each carry a permanent dipole moment and tend to align themselves in a way such that the bulk dipole moment is vanishing.[3] This project will strictly focus on the nematic to isotropic phase transition due to heating and the isotropic to nematic phase transition due to cooling.

Some other phases that liquid crystals exhibit are cholesteric phases or also known as chiral nematic phases. In this phase two dimensional disks of nematic like structures stack together with each disk slightly twisted with respect to the one above it creating an overall helical structure. There are also smectic phases which have a higher order than the nematic phase and in turn are more solid like than the nematic phase. Smectic phases also show translational order. The word smectic is derived from the Greek word for soap because of its soapy visual appearance.[2] In smectic phases molecules usually form layers or planes and the molecules are free to move within the layers and move less freely between layers. Separate planes or layers can move with respect to each other. Within each two dimensional plane or layer the liquid crystal is basically in the nematic phase.[15] There are a rich variety of smectic phases. For more detailed information on cholesteric and smectic phases see DeGennes The physics of Liquid crystals.

Solid crystalline phase is the highest ordered phase where the order parameter is equal to one. This phase occurs at lower temperatures in comparison with the other phase temperatures. The

structure is no longer fluid like and the molecules may only vibrate in position and they cannot move freely. The crystal is characterized by a three dimensional arrangement of atoms that are repeated over and over. A typical crystal structure can be seen in Figure 5.

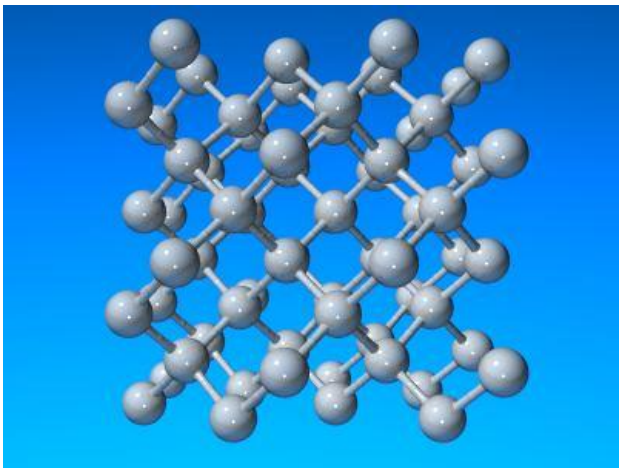

Figure 5 Crystal structure of diamond[16]

1.6 5CB

5CB or 4'-n-pentyl-4-cyanobiphenyl is a thermotropic liquid crystal which only has one liquid crystalline phase, the nematic. It is a rod-like geometrically anisotropic mesogen that transitions from a solid crystal to the nematic phase at about 22.5^{o} C and transitions from nematic to isotropic at about 35^{o} C. The latent heats released or absorbed in those transitions is 17.2 kJ and .8 kJ respectively.[17] The transitions between these phases are enantiotropic, they are reversible upon heating and cooling.[17] 5CB consists of 18 carbon molecules, 19 hydrogen molecules, and one nitrogen molecule. A 5CB molecule is approximately 20 angstroms long and 5 angstroms wide at the equatorial center. 5CB also has a strong longitudinal dipole moment.[17] A picture of its molecular structure can be seen below in figure 6.

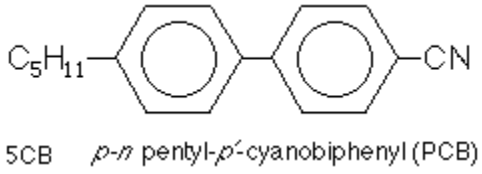

Figure 6 5CB Molecule[18]

5CB has a molecular weight of 249.4 g/mole and a density of about 1 gram per centimeter cubed.[19] Because 5CB is without a central linking group it is one of the most stable liquid crystals ever synthesized which makes it one of the most studied.[3]

1.7 Buckministerfullerene C_{60}

A fullerene is defined as a molecule composed entirely of carbon. They can take the shape of a sphere(ball), line (wire), ellipsoid(egg), or cylinder(tube). Common fullerenes include buckyballs and carbon nanotubes. Fullerenes are carbon allotropes; others include diamond, graphite, and charcoal. Buckyballs also known as buckministerfullerene or C_{60} consists, of 60 carbon atoms which are linked together and resemble a soccer ball. It was named after R. Buckminster Fuller because the nanostructure resembled the geodesic domes he created as an architect.[20] A C_{60} molecule is a truncated icosahedron with twelve pentagons and twenty hexagons, with each polygon edge consisting of a bond and each vertex consisting of a carbon molecule.[21] Each carbon molecule is covalently bonded to three other adjacent carbon atoms.[20] A C_{60} molecule can be seen below in Figure 7.

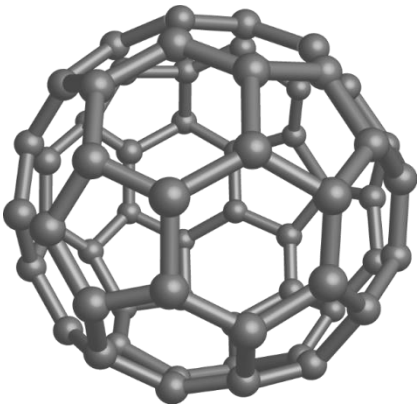

Figure 7 C_{60} fullerene[22]

The Van der Waals diameter of C_{60} is approximately 1 nanometer, the nucleus to nucleus diameter is about .7 nano-meters, and the average bond length is around 1.4 angstroms. C_{60} is the most common fullerene found in nature and is observed in small amounts soot or smoke from certain forms of carbon. C_{60} is the only known carbon allotrope to be soluble.[23] C_{60} was first theorized in 1970 by Eiji

Osawa of Toyohashi University of Technology and first observed in 1985 using mass spectrometry.[24] Buckyballs have some unique characteristics; they are roundest most symmetrical molecule known to man which makes them very resistant to high speed collisions. The buckyball can withstand slamming into a stainless steel plate at 15,000 mph and just bounce back with no damage and when compressed to 70 percent of its original size the buckyball becomes more than twice as hard as diamond.[25] C_{60} is the largest and most complex molecule to date that was experimentally shown to have a DeBroglie wavelength which shows its inherent wave-particle duality. The C_{60} molecule is also extremely stable and since carbons atoms are only bonded to other carbon atoms the molecule is very inert. The bonds have a property called aromaticity, meaning the electrons can move freely between the bonds.[23] C_{60} molecules cannot bond to other C_{60} molecules however they do stick together on account of Van Der Waals forces. C_{60} has many potential applications because it's unique physical properties. Some of the physical characteristics of C_{60} can be seen in Figure 8.

C_{60} Properties

Average C-C distance	1.44 Å
FCC Lattice constant	14.17 Å
C60 mean ball diameter	6.83 Å
C60 ball outer diameter	10.18 Å
C60 ball inner diameter	3.48 Å
Tetrahedral site radius	1.12 Å
Octahedral site radius	2.07 Å
Mass density	1.72 g/cm3
Molecular density	1.44 x 1021/cm3
Compressibility (-d in V/dP)	6.9 x 10-12/cm3/dye
Bulk modulus	14 Gpa
Structural phase transitions	255K, 90K
Binding energy per atom	7.4 eV
Electron affinity (pristine C60)	2.65 eV
Ionization potential (1st)	7.58 eV
Ionization potential (2nd)	11.5eV
Vol. Coeff. Of thermal expansion	6.2 x 10-5 cm3/K
Band gap (HOMO-LUMO)	1.7 eV
Spin- orbit splitting C (2p)	0.0022 eV
Velocity of sound vt	2.1 x 105 cm/sec
Velocity of sound vl	3.6 x 105 cm/sec
Debye temperature	185 K

Thermal conductivity (300 K)	0.4W/mK
Phonon mean free path	50 Å
Static dielectric constant	4.0 – 4.5
Standard heat of formation	9.08 k cal mol-1
Index of refraction	2.2 (600nm)
Boiling point	Sublimes at 800K
Resistively	1014 ohms m-1
Vapor density	N/A
Vapor pressure	5 x 10-6 torr at room temp.

Figure 8 Properties of C_{60}[26]

1.8 Recent research in 5CB Fullerene composites

A recent study was performed testing the properties of 5CB liquid crystal and multiwalled carbon nanotube (MWCNT) 5-30 nm in diameter and 1-5 μm in length composites. The nematic to isotropic phase transition of weight concentrations 0.05, 0.1, 0.15, 0.2, 0.25, and 0.3 percent MWCNT in a 5CB medium were studied electrically and thermodynamically using the technique of dielectric spectroscopy and AC calorimetry respectively. Both experimental techniques suggested that the MWCNT dispersed in the 5CB created a local lyotropic pseudo-nematic phase but this does not change the net energy fluctuation in the isotropic to nematic phase transition. This lyotropic pseudo-nematic phase may be caused by the MWCNT aggregation, due to the 5CB molecules anchoring to the outside of the nanotube wall and Van Deer wals forces between the MWCNT, which create local isolated short range orientation orders.[27]

2. Methods

2.1 Sample preparation

The goal of the sample preparation was to make the dispersions of C_{60} as homogenously dispersed throughout the 5CB as possible and make all composites the same way without any contamination. The first step of preparing the composite samples was to clear the lab area and remove all foreign dirt and dust that would contaminate and samples. The glass vials to put the samples in and the lab spoons used to scoop the materials with were first cleaned with purified water and placed on the hot plate at 50 degrees Celsius for approximately a half hour, the glass containers and instruments were then cleaned with pure acetone and again placed on the hot plate for approximately an hour at 50 degrees Celsius.

Next the scale was calibrated and the materials were weighed out. The method was a container would be weighed out and after the scale had zeroed the glass vial would be reweighed after some liquid crystal was placed inside. The new mass minus the mass of the glass container empty would yield the mass of the liquid crystal.

$$Mass\ of\ Liquid\ Crystal = Total\ Mass - Mass\ of\ empty\ container$$

The liquid crystal mass would then be multiplied the percentage of the composite being made and that mass would be the mass of the C_{60} which was to be weighed out and mixed with the 5CB to make the composite.

$$Mass\ of\ \mathrm{C}_{60} = Mass\ of\ Liquid\ Crystal * (composite\ percentage)$$

A new piece of sterile non-stick wax paper was placed on the scale, the scale was zeroed, then the C_{60} was scooped onto the paper until the desired amount was weighed. The C_{60} was then placed inside the glass container holding the liquid crystal.

A liberal amount of pure acetone was squeezed into the mixture to dilute and enable an easier, more uniform, diffusion of the C_{60} molecules into the bulk liquid crystal. The container cap was screwed on and the container was manually shaken up and placed in the sonic vibrator over night. The container was then placed on the hot plate at 50 degrees Celsius over night with the cap off to evaporate the acetone. To ensure that all traces of the acetone and moisture were gone the composite sample was degassed by being placed on the hot plate at 40 degrees Celsius and slowly put under vacuum for approximately 2 hours. The cap was then screwed back onto the container put in storage until the experimentation was ready. Before the sample was placed into any cell the container was placed on the mechanical vibrator for approximately 10 minutes to ensure homogeneity.

2.2 Modulated Differential Scanning Calorimetry (MDSC)

2.2.1 Introduction to Modulated Differential Scanning Calorimetry

A differential scanning calorimeter is an experimental devise which heats/cools a sample material with a linear heat ramp while measuring the heat into or out of the sample relative to a reference.[28] While a modulated differential scanning calorimeter overlays a sinusoidal temperature oscillation on the traditional DSC linear heat ramp, see figure 9.[29]

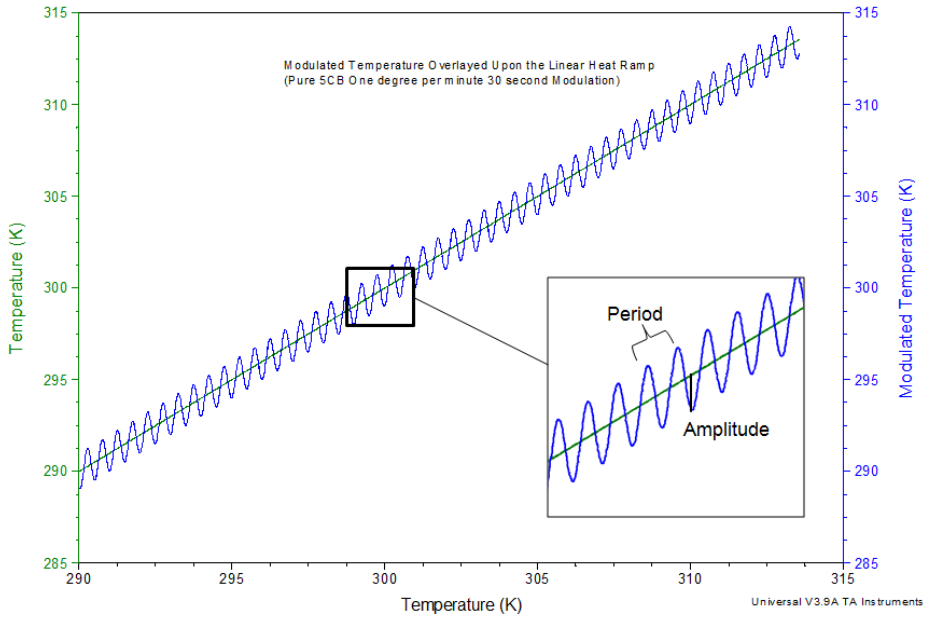

Figure 9 Modulated Temperature superimposed on Average Temperature Rate

The linear ramp rate provides the total heat flow rate and the sinusoidal modulated heating rate is used to determine the part of the total heat flow rate that responds to a change in heating rate. This part of the heat flow rate is generally caused by the heat capacity or a change in the heat capacity.[30] One of the disadvantages of the traditional DSC machine is that it is not possible to maximize sensitivity and resolution in one experiment. In a DSC machine, to increase the sensitivity of detecting transitions within the sample one must increase in crease sample size or ramp rate or both. This increased sensitivity will decrease resolution because both the increase in sample size and ramp rate will cause a larger temperature gradient within the sample. MDSC can have both high sensitivity and high resolution in the same experiment because of its two simultaneous heat rates. The average heating rate can be slowed to improve resolution while the modulated heating rate can be high to improve sensitivity.[28] Traditional DSC can only measure the average heat flow rate of any process which makes any individual process undistinguishable. By introducing a modulated heating rate along with a linear heating rate MDSC can measure the components of the heat flow and individual processes can be identified. This feature of MDSC is valuable when experimenting on blends of materials or composites.[31] It is important

to point out that the average value of the modulated heat flow signal is equal to the heat flow signal from the conventional DSC at the same average heating rate. The average value of the modulated heat flow signal is found by the software continuously performing a fast Fourier Transformation analysis calculated every .1 seconds instead of a simple overall average which would limit the result.[28,32]

Inside the Q200's measuring chamber nitrogen is used as a purge gas. The reasons for a purge gas flow is the gas helps to eliminate moisture and oxygen which could damage a cell over time, it creates a consistently uniform temperature inside the measuring chamber which helps to remove any localized hot-spots which could cause errors in the data, the purge gas helps create more efficient heat transfer between constantan alloy disk and sample cell which results in increased sensitivity and response time, it also helps to cool the cell which can make the cooling rates faster and allows for a wider modulation to be used. The nitrogen flow rate used was approximately 50 ml/min. The purge gas was mainly used as a way to optimize the MDSC's experimental results by making the data more accurate and reproducible.[33] The instrument used for experimentation was TA Instrument's DSC model Q200, pictured in Figure 10, which can also operate as a MDSC.

Figure 10 Q200 MDSC[34]

2.2.2 Theory

The MDSC signals are derived by three measurements the machine observes: time, the stimulus modulated temperature, and the response modulated heat flow. The signals modulated heat flow and

modulated heating rate are the only signals measured by the MDSC machine all others are calculated by the machine using the two original signals.[30]

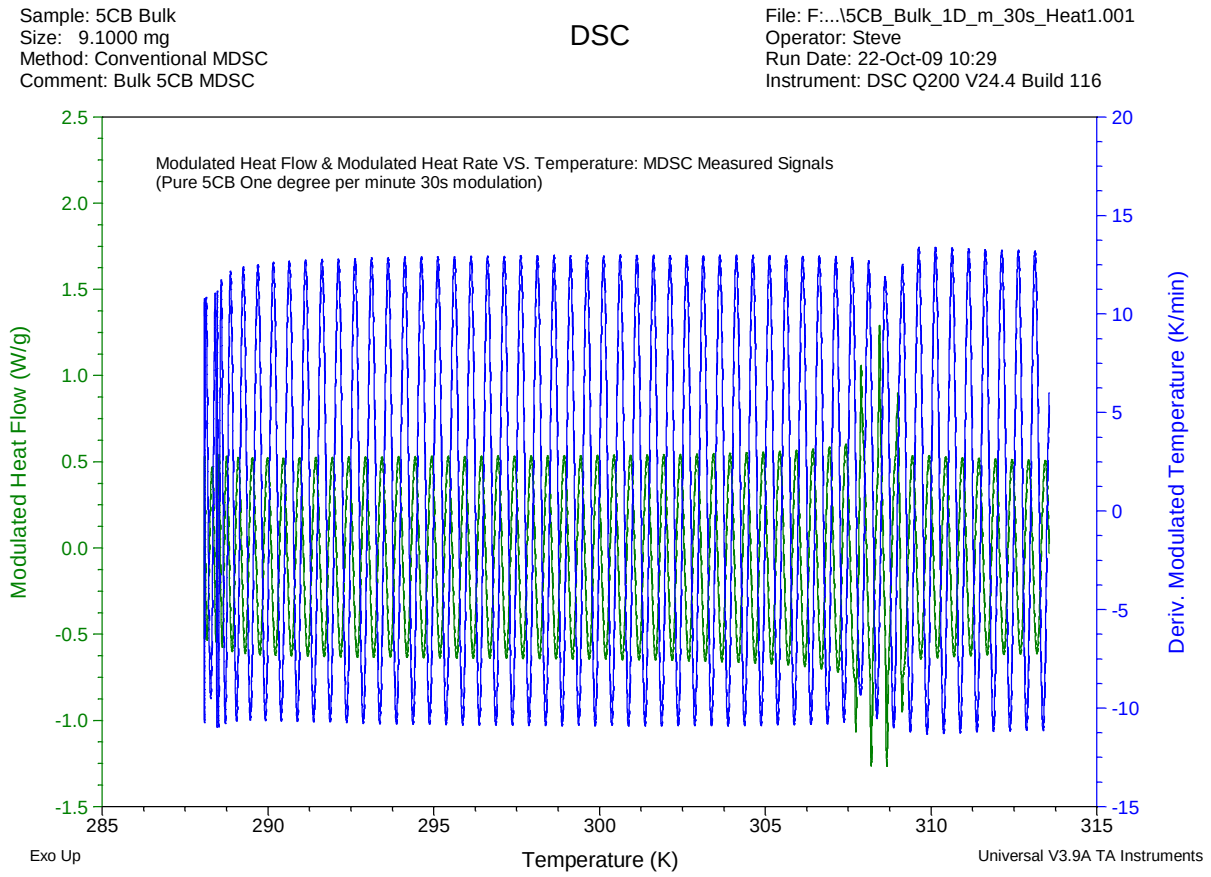

Figure 11 MDSC Raw Signals

The quantities are related in the equation,

$$\frac{dH}{dt} = C_p \frac{dT}{dt} + f(T,t)$$

Where $\frac{dH}{dt}$ is the total heat flow measured by the calorimeter, C_p is the specific heat capacity, $\frac{dT}{dt}$ is the heat rate stimulated by the machine, and $f(T,t)$ is the kinetic response of the sample also known as the nonreversing part of the heat flow. The nonreversing part is the heat flow that is a function of time at an absolute temperature.[28] In this case the specific heat is equal to,

$$C_p = \frac{Amplitude\ of\ modulated\ heat\ flow}{Amplitude\ of\ modulated\ heating\ rate} * K$$

where K is the Heat capacity calibration factor. The heat capacity calibration constant is determined by taking the ratio of the cell materials theoretical capacity over the measured heat capacity of the material.[28] The MDSC machine measures the total heat flow and heat capacitance while it produces the constant heating rate through temperature modulation. The machine measures signals from the sample cell and reference cell independently and subtracts their values to obtain the correct signal for the sample itself. The way the total heat flow is measured and calculated can be seen in the flow chart provided in Figure 12.

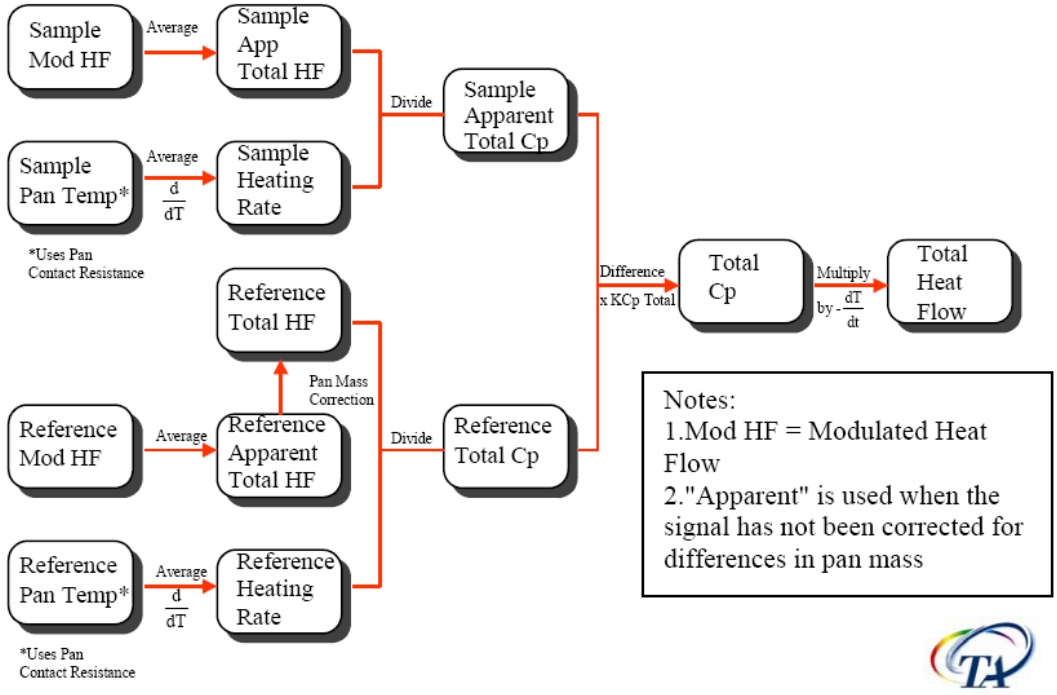

Figure 12 Flow Chart of MDSC Total Heat Flow Derivation[35]

The method for calculated the reversing heat flow can be seen in the flow chart in Figure 13.

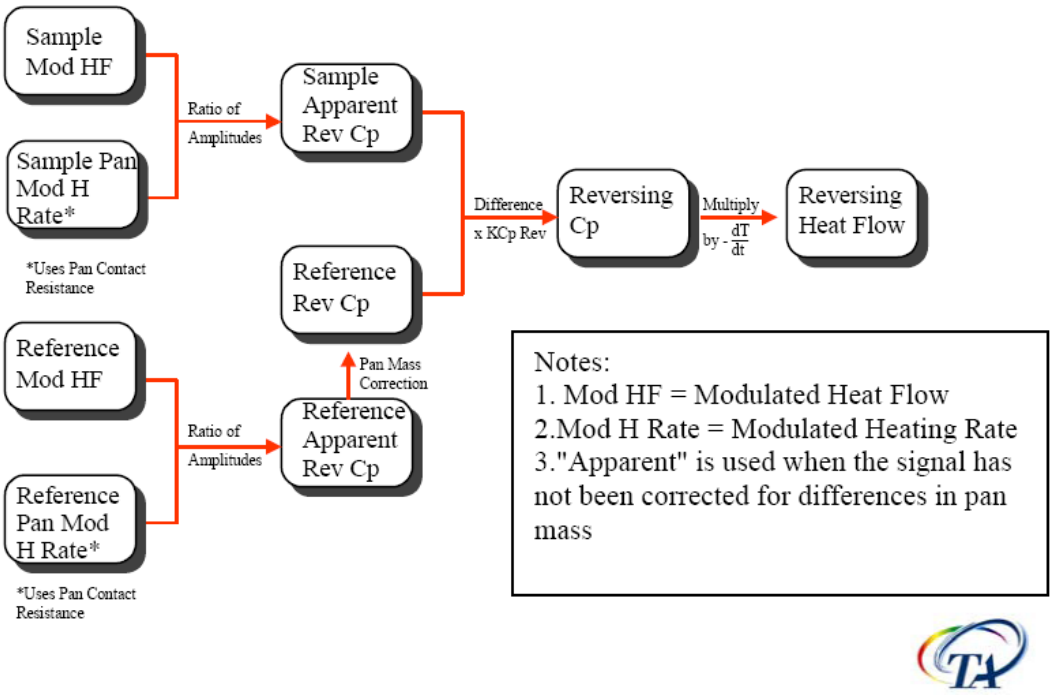

Figure 13 Flow Chart of MDSC Reversing Heat Flow Derivation[35]

To obtain the kinetic part of the heat flow $f(T,t)$ the machine then subtracts the total heat flow by the reversing heat flow.

$$f(T,t) = \frac{dH}{dt} - C_p \frac{dT}{dt}$$

The term in the equation, heat capacitance multiplied by the heating rate, is also considered the reversing heat flow and the kinetic term is considered the nonreversing heat flow. Although the heat flow terms are known as reversing and nonreversing MDSC tells nothing about whether a phase transition is reversible or nonreversible. The term was named reversing because true heat capacity, the heat associated with increasing or decreasing a materials temperature, is reversible. A change in heat capacity due to a transition will show up on the reversing signal, but the process may or may not be reversible.[31]

2.2.3 Experimentation

There were numerous samples tested in the MDSC Q200 to see the effect of different concentrations of C_{60} dispersed into 5CB on the nematic to isotropic and isotropic to nematic phase transitions. The composite concentrations tested were pure 5CB, 5CB with a 1% C_{60} concentration, 5CB with a 2% C_{60} concentration, 5CB with a 5% C_{60} concentration, 5CB with a 10% C_{60} concentration, 5CB with a 25% C_{60} concentration, 5CB with a 50% C_{60} concentration, and finally pure C_{60}. A large difference in the observed phenomena occurred between 10%-25% so extra testing of concentrations of 15% and 20% C_{60} were performed. The phase transitions for pure 5CB are well documented but for experimental consistency the pure liquid crystal that was to be made into composites was tested. The pure C_{60} does not experience a phase transition in the range being tested (approximately 285K to 315K) but nevertheless it was tested in the same manner as the composites.

The samples were tested with a heat and cool at scan rates of .5 Kelvin per minute, 1 Kelvin per minute, 2 Kelvin per minute, and 3 Kelvin per minute with a 30 second modulation period. The multiple scan rates were used to see if any scan rate dependence is present and to see if there are any anomalies in the data. The samples were also tested with a heat and cool under different modulation periods of 30 seconds, 60 seconds, 75 seconds, and 100 seconds at a scan rate of .5 Kelvin per minute. The different frequencies were used to see if any frequency dependence exists and to make sure no anomalies are present. The main MDSC signals analyzed were the reversible and nonreversible components of the heat capacity to determine the nature of the nematic to isotropic phase transition.

2.3 Polarizing Microscopy

Polarized microscope images were taken of each weight concentration of C_{60} to see how the two molecules are arranging themselves on a microscopic level and to gain more insight into their thermodynamical behavior. A polarized light microscope uses polarized light to illuminate a magnified image of something on the micro scale. It is an optical tool well suited for probing the structure of

anisotropic materials due to their birefringence. Since light is considered a transverse electromagnetic wave, electric and magnetic fields oscillate perpendicular to the propagation direction of the light wave, it can be polarized. Polarization is a property of waves that describes their orientation of oscillation and can be characterized by the difference in the oscillating waves' phases. Linear polarized light has electric and magnetic components in phase, their maximum and minimum are reached at the same time which means their vector sum leads to one wave resulting in a polarization of 45 degrees. When the field components are 180 degrees out of phase the result is a linearly polarized light wave 45 degrees in the opposite direction. When the wave components are 90 degrees out of phase the light becomes circularly polarized, one wave is at a maximum while the other is at a minimum. The most general case is when the wave components are out of phase at an arbitrary angle that isn't 90 or 180 degrees, the resultant is an elliptically polarized light wave.[36] The type of light used in the microscope experimentation was ordinary white light which is made of waves that fluctuate at all possible angles. A figure of a similar polarized light microscope can be seen below.

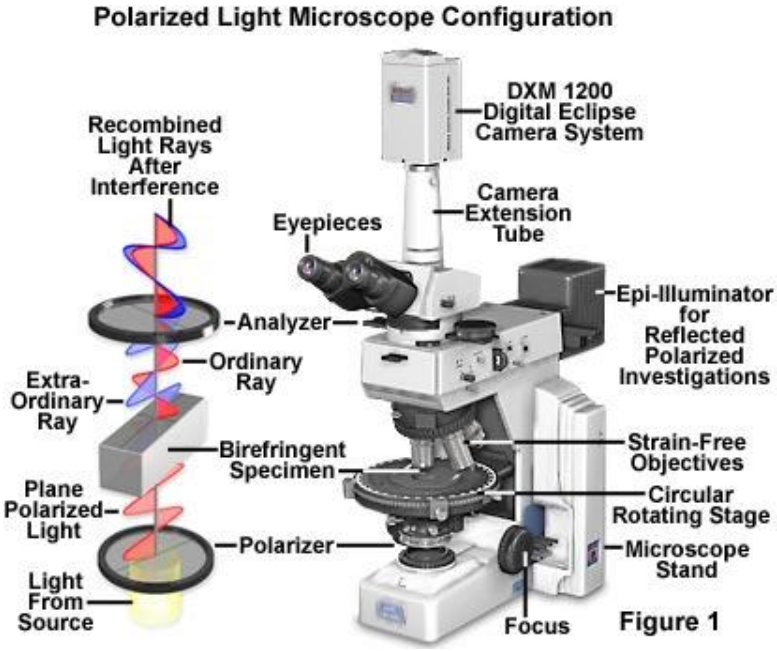

Figure 14 Example of Microscope Set-up[36]

The cartoon on the left-hand side of the figure shows the inner workings of a polarized light microscope. White light is produced at the source and that white light first goes through a polarizer. A polarizer is a material that allows light of only a certain angle to pass through. If the polarized light is then sent through another polarizer of the same angle the light will pass through freely but if the second polarizer is perpendicular to the first, known as a crossed polarizer (analyzer), no light will be allowed through. As the angle of the second polarizer rotates from 0 to 90 degrees less light will be transmitted through.[37] See figure 15.

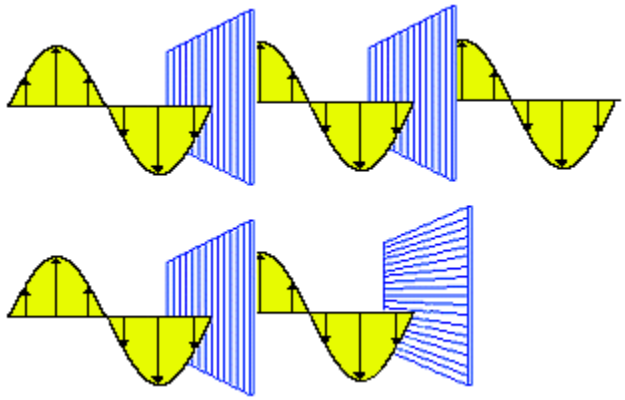

Figure 15 Relationship of Polarizers and Polarized Light[37]

After the light becomes initially polarized it then transverses the birefringent liquid crystal specimen. The liquid crystal is birefringent because of its anisotropic nature. When light passes through birefringent materials it experiences double refraction due to the liquid crystal having two indices of refraction. An index of refraction is a ratio of the speed of light in a vacuum over the speed of light in some medium. The reason the birefringent liquid crystal has two indices of refraction is because the two wave components of the light are each polarized in mutually perpendicular planes so one component of the light wave will travel faster through the material than the other. The fast component is called the ordinary ray and slow component is called the extraordinary ray. Once these two components pass through the liquid crystal they then pass through a crossed polarizer 90 degrees to the first called the

analyzer. With no specimen in the microscope the image appears black because the two polarizers are perpendicular and no light is allowed to pass through. Since the birefringent liquid crystal caused the two light components to travel at different speeds the light wave becomes out of phase which changes its polarization state and as the wave passes through the analyzer the two components are recombined with constructive and destructive interference allowing structure of the specimen to be observed. The birefringence of the liquid crystal is described by the difference in the indices of refraction Δn.[38]

$$\Delta n = n_e - n_o$$

Where n_e is the index of refraction for the extraordinary light ray and n_o is the index of refraction of the ordinary light ray. The birefringence of 5CB in the human visible spectrum is between .11 to .2 depending on temperature and light wavelength and the index of refraction of C_{60} is 2.2.

2.4 Mechanically Quenched Steric Model

A macroscopic model of each weight concentration was created using white pipe cleaners to represent liquid crystal molecules and using black "pom-pom" balls to represent C_{60} molecules to test the steric behavior of how the molecules pack together according to their unique geometries. The pipe cleaners were approximately cylindrical with a diameter of approximately .5 cm and were cut to 2 cm lengths. The "pom-pom" balls were approximately spherical and had a diameter of 1 cm. The dimensions of the pipe cleaners liquid crystals and pom-pom buckyballs allow for a scaling factor of 1 cm in the model representing 1 nm. The weight percentages of the different composite concentrations were converted into percents of C60 molecules in each solution and volume of C_{60} in each solution using the densities and molar masses, see figure 16.

C60 weight %	C60 volume %	C60 molecule %	# of model C60 molecules per 500 5CB molecules
1%	0.587	0.349	1.75
2%	1.187	0.706	3.53
5%	3.060	1.821	9.11
10%	6.460	3.844	19.22
15%	10.260	6.106	30.53
20%	14.535	8.650	43.25
25%	19.380	11.533	57.67
50%	58.140	34.600	173

Figure 16 Table of C_{60} Weight Percentage Conversions

Five hundred model liquid crystal particles were placed on a pan roughly in the same direction to represent the nematic phase and the appropriate amount of model C_{60} molecules were placed on top. The pan was lightly shaken to represent a mechanical disturbance such as the sonic bath or mechanical vibrator used in the mixing process of the samples or an increase in temperature. A thermal quench was represented by abruptly stopping the mechanical disturbance allowing the geometrical packing of the molecules for different concentrations to be observed several times. Multiple images were taken using a box to mount the camera above model keeping the same it in the same position. The box had a viewing window cut into the top where the camera was mounted. It should be noted that this model has some error due to the fact that not all the pipe cleaners may have been the exact length, the pom-pom balls were sometimes misshapen and not perfectly spherical, a liquid crystal molecule isn't cylindrical it is rod-like, and the buckyballs are not perfect spheres they are truncated icosahedrons.

3. Results

3.1 MDSC Results

The different concentration's reversible and nonreversible heat capacitance signals were all compared at different scan rates to see the effect of different average heating/cooling rates. From the reversible heat capacitance curve three quantities can be determined peak temperature (a bit of a misnomer the peak temperature is the temperature where the reversible heat capacitance peaks), enthalpy or the amount of energy transferred during the transition process, and the full width at half maximum of the reversible heat capacitance curve. If the integral of the reversible heat capacitance signal is taken with respect to temperature with a proper baseline the area yields the heat energy required for the phase transition or in other words the enthalpy.[28] The full width at half max, measured as a temperature range, gives vital information about the phase transition, the larger the full width at half max, the broader the peak, the larger the coexistence of both nematic and isotropic phase domains within the sample during the phase transition. For example when boiling water the water doesn't turn instantly to steam but when boiling there is both water and gas bubbling within it which is the existence of both the liquid and gaseous phase, this is similar to what is happening with the liquid crystal phase transition between nematic and isotropic. An example of bulk 5CB at a .5 K/min temperature ramp rate and a 30 second temperature modulation with all three quantities (peak temperature, enthalpy, Full Width At Half Max) can be seen in figure 17.

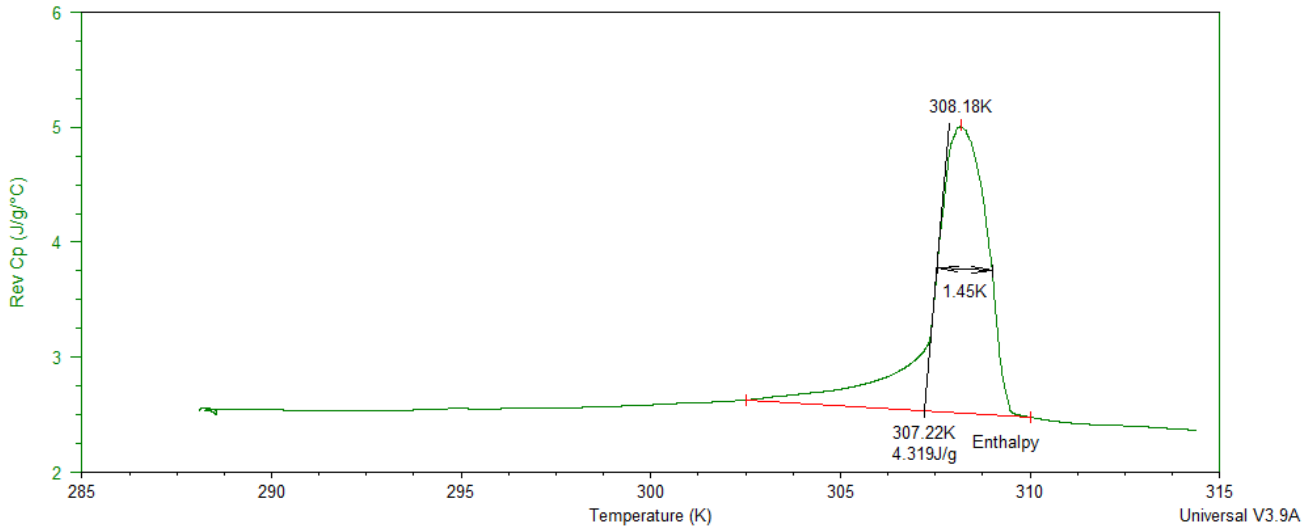

Figure 17 Pure 5CB .5 K/min 30s (Peak Temperature, Enthalpy, Full Width at Half Max)

3.1.1 Scan Rate .5 K/min Temperature Modulation 30s

The .5 degree per minute temperature ramp was the slowest ramp rate used in experimentation. All scan rate dependence .5, 1, 2, 3 K/min were run with a 30s temperature modulation. Figure 18 shows the reversible heat capacitance for all concentrations at .5 Kelvin per minute. The figure shows many reoccurring trends that hold for all other scan rates and temperature modulation periods. For one the bulk curve is always farthest to the right yielding the highest peak temperature, the 25% curve usually ends up far to the left of all other curves yielding the lowest peak temperature, 2%,5%, and 10% were most the time very similar and slightly shifted to the left of the bulk. The 1% concentration could be random at times but as in figure 18 many times was close to 2,5, and 10 % but the 1% curves were always far enough away to be considered anomalistic. The 50% curve exhibited wildly fluctuating behavior. In many instances the peaks would be much greater than all others and many times 50% concentration would appear to act like bulk 5CB. The concentrations of 15% and 20% were done after all the others had been done in hopes of finding reversible curves that would show a trend to lower the transition temperature on a path towards the 25% peak temperature, however like the 50% concentration these two fluctuated wildly and seemingly randomly.

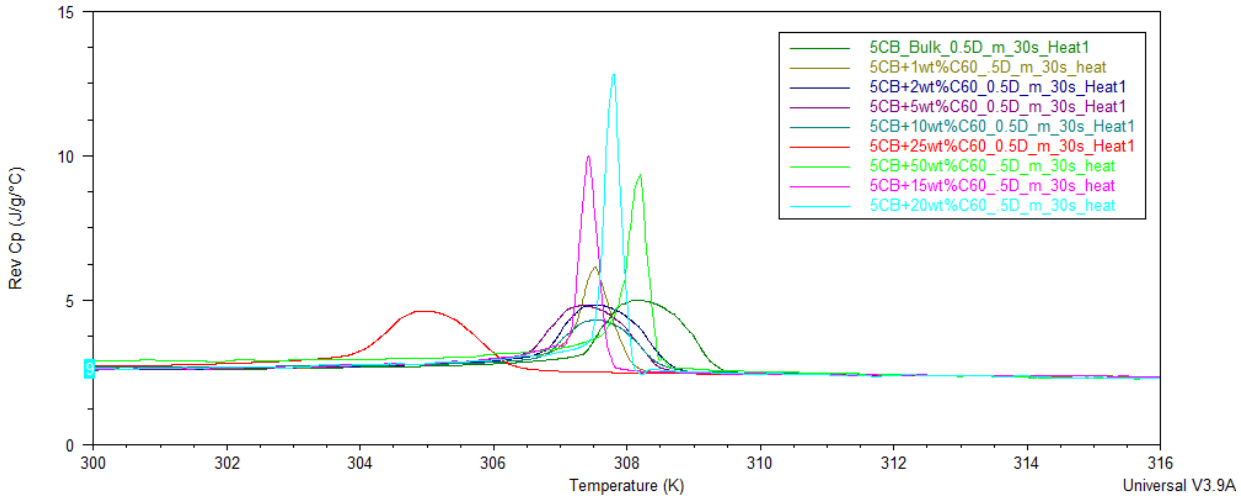

Figure 18 Reversible Cp .5 K/min (heat)

The reversible heat capacitance during the cool, seen in figure 19, is very similar to the heat except the 50% curve has a much larger peak which is typical trend seen most other scan rate and frequency scans.

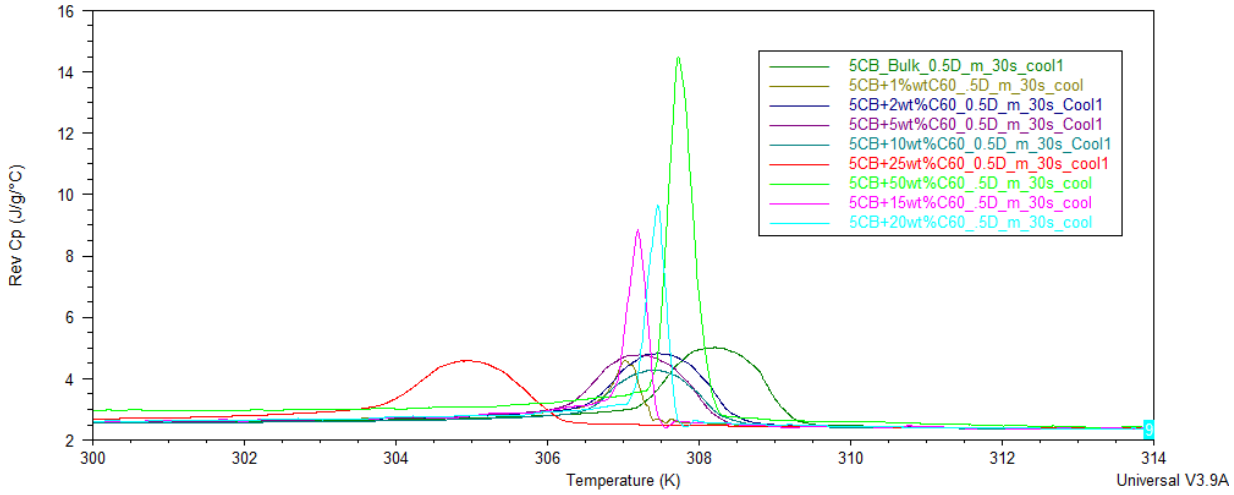

Figure 19 Reversible Cp .5 K/min (cool)

The nonreversible signal shows the change in heat capacitance due to kinetic processes within the sample and the expectation was to see the bulk curve mimicked except shifted to the left and broadened out as concentration increases until a critical concentration is reached and the 5CB becomes over saturated with C_{60} molecules. The nonreversible signal does show shifts to the left of the curves like the reversible sign. The concentrations many times mimic the shape of the bulk curve and the 25% curve

is always way to the left and fairly broad. Like the reversible curves 2,5, and 10 percent are all every similar and fluctuation around each other's values and 1% , 15%, 20% and 50% all show some random behavior such as large peaks, curves that go the wrong way (like the 20% curve in figure 20), large shifts in behavior between heats and cools, scan rates, and/or temperature modulation.

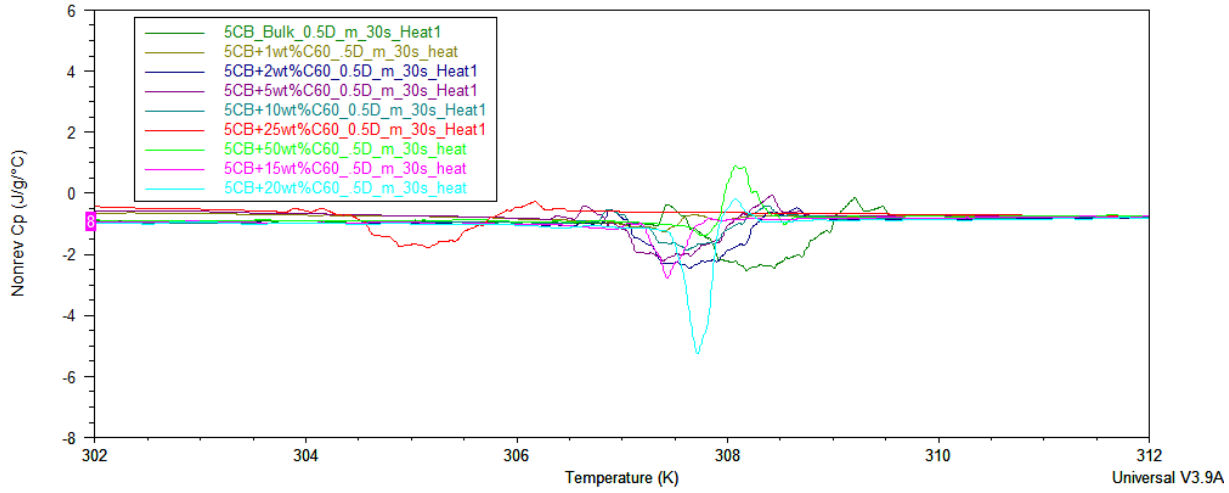

Figure 20 Nonreversible Cp .5 K/min (heat)

The nonrversible heat capacitance cool at .5 K/min, seen in figure 21, shows odd behavior from the concentrations 1%, 15%, 20%, and 50%.

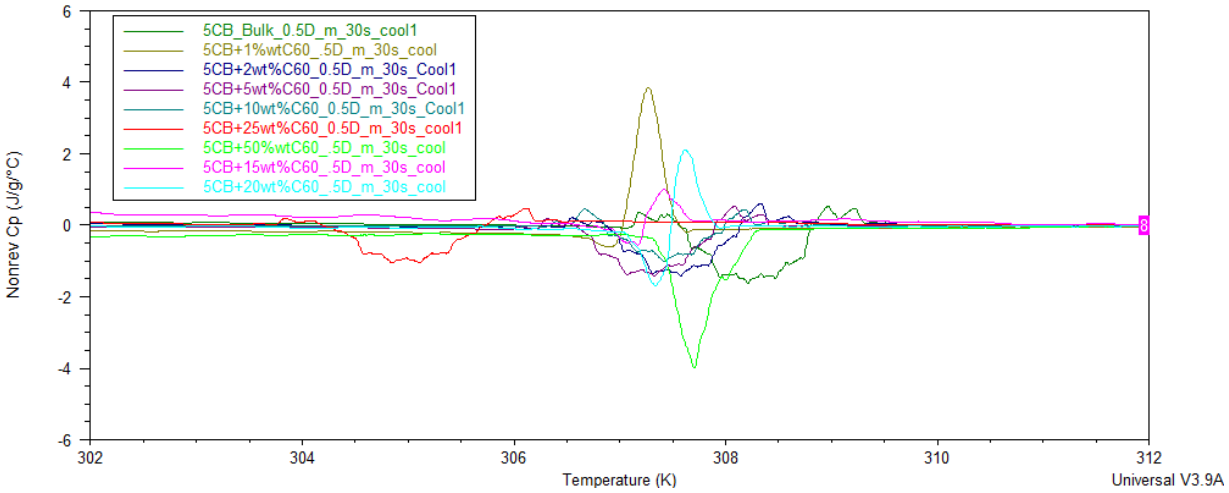

Figure 21 Nonreversible Cp .5 K/min (cool)

The reversible curves and nonreversible heat capacitance curves for the other faster scan rates 1, 2, and 3 degrees per minute as well as all different temperature modulations 45s, 60s, 75s, and 100s followed the trends described above for the .5 K/min average temperature ramp. Their reversible and nonreversible heat capacitance heat and cool graphs can be found in Appendix A and B.

3.1.2 Scan Rate Peaks

While examining the temperature that the reversible heat capacitance peaks during heats and cools, in figure 22 and 23, there are a few significant trends. One is that the highest temperature is always for the bulk liquid crystal. Percentages between bulk and 25% are all fairly similar and seem to fluctuate. At 25% there is a significant drop in the temperature peak, this is representative of the far shirt to the left of its reversible heat capacitance curves. The 50% concentration peak temperatures rise back almost to the bulk value. These peak temperatures don't appear to show any scan rate dependence and the heat and cools are very similar. A table showing the actual number values represented in the peak temperature figures 22 and 23 can be found in Appendix C.

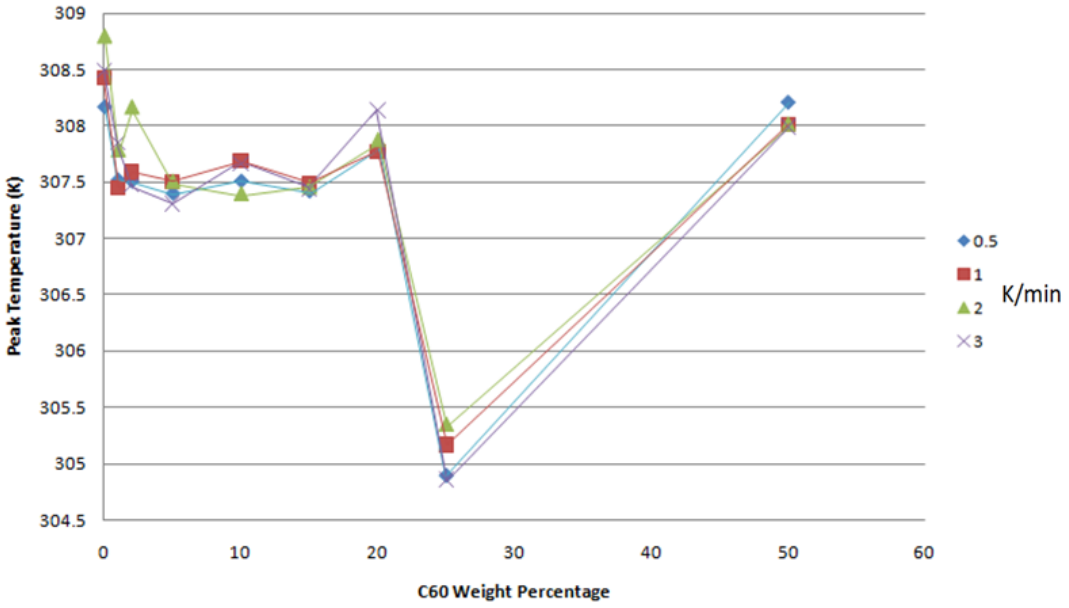

Figure 22 C_{60} Peak Temperatures as a function of temperature ramp rate (heat)

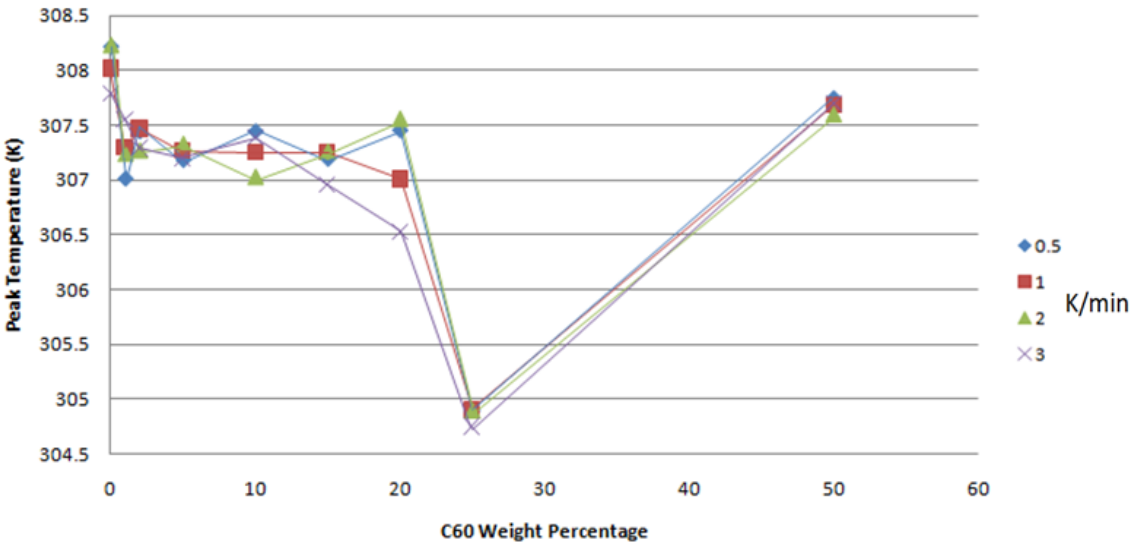

Figure 23 Peak Temperatures as a function of temperature ramp rate (cool)

3.1.3 Scan Rate Enthalpy

The enthalpy of nematic to isotropic phase transition seemed to be totally random, see figure 24. There was no scan rate dependence and the different concentrations fluctuated wildly. The 1% concentration usually always had the lowest enthalpy. Many times because of the large peaks in 50% reversible curve its enthalpy appears much higher as can be seen in figure 25. A table showing the actual number values represented in the enthalpy in figures 24 and 25 can be found in Appendix D.

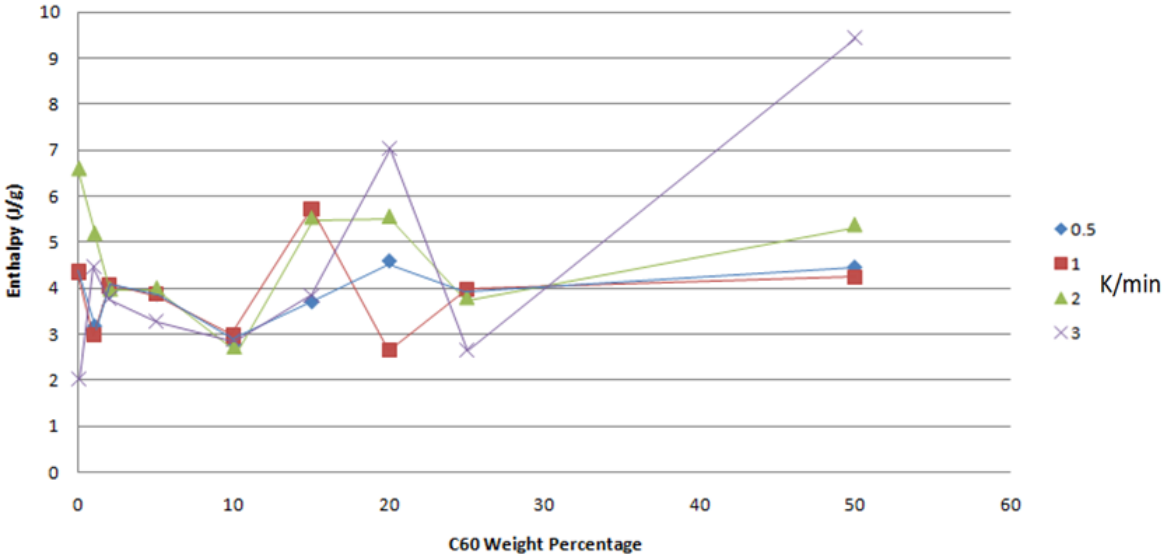

Figure 24 Enthalpy of phase transitions as a function of temperature ramp rate (heat)

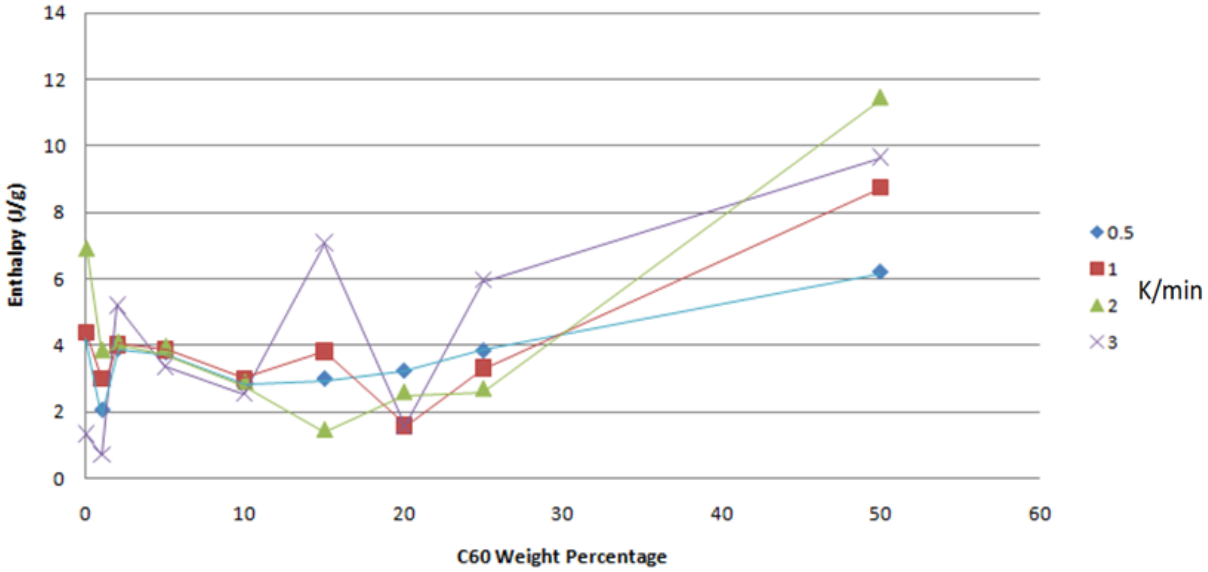

Figure 25 Enthalpy of phase transitions as a function of temperature ramp rate (cool)

3.1.4 Scan Rate Full Width At Half Max

The full width at half max of the reversible heat capacitance peak seen in figure 26, representing the coexistence of nematic and isotropic phases during the phase transition, seems to get larger for most concentrations as the temperature ramp rate becomes faster showing some dependence on scan rate. The 1% concentration did have a consistently small full width at half max. These were the only

significant trends, other than them the full width at half max seemed to vary a lot. The heat and cools also showed a decent amount of difference between one another. A table showing the actual number values represented in the full width at half max figures 26 and 27 can be found in Appendix E.

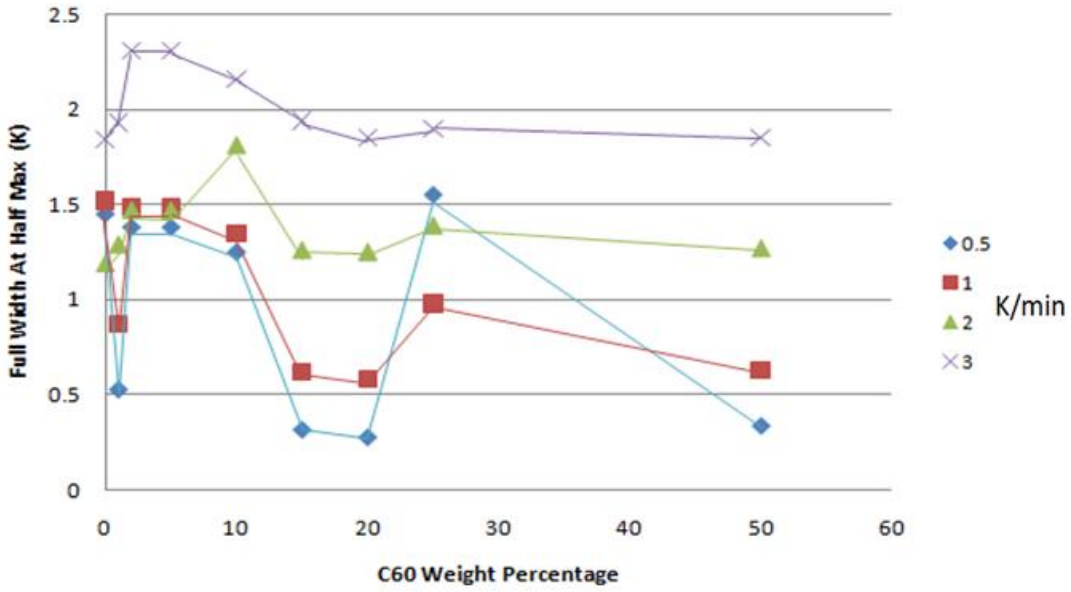

Figure 26 Full Width At Half Max of C_{60} concentration's reversible heat capacitance signal peak as a function of temperature ramp rate (heat)

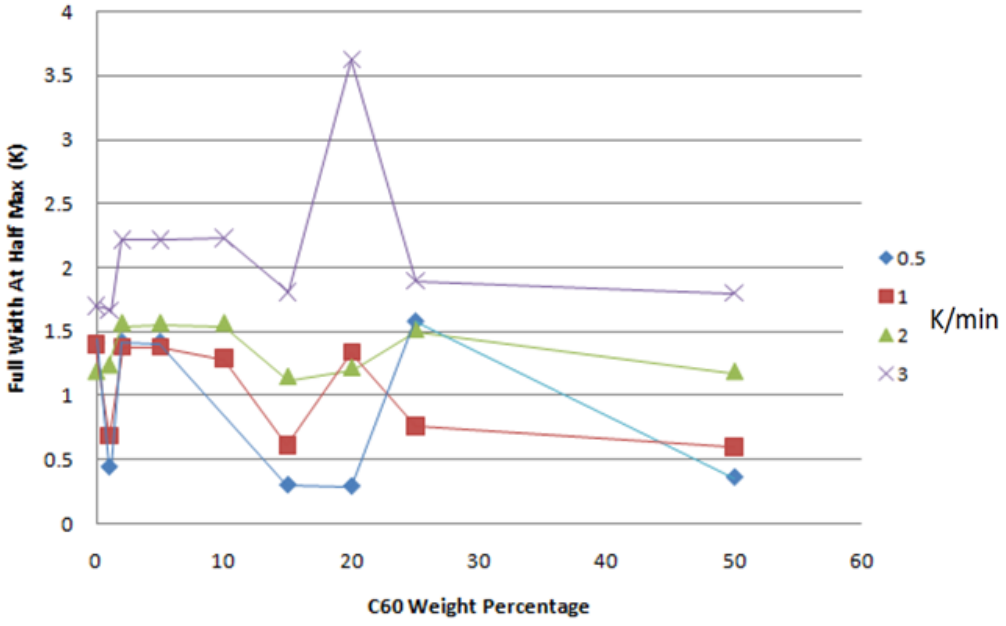

Figure 27 Full Width At Half Max of C_{60} concentration's reversible heat capacitance signal peak as a function of temperature ramp rate (cool)

3.1.5 Frequency Peaks

The temperature of the reversible heat capacitance heat and cool peaks at different temperature modulations, which can be seen in figure 28 and 29, seem to be very similar to that of the comparison of the different scan rates. The bulk 5CB gives the highest peak temperature as expected, there is a minima at 25%, and 50% seems to trend back towards the bulk values. The concentrations of 15% and 20% have no frequency dependent data because they were done after the initial testing with only a scan rate dependence due to time constrictions. The peaks don't show a significant frequency dependence. A table showing the actual number values represented in the peak temperature figures 28 and 29 can be found in Appendix C.

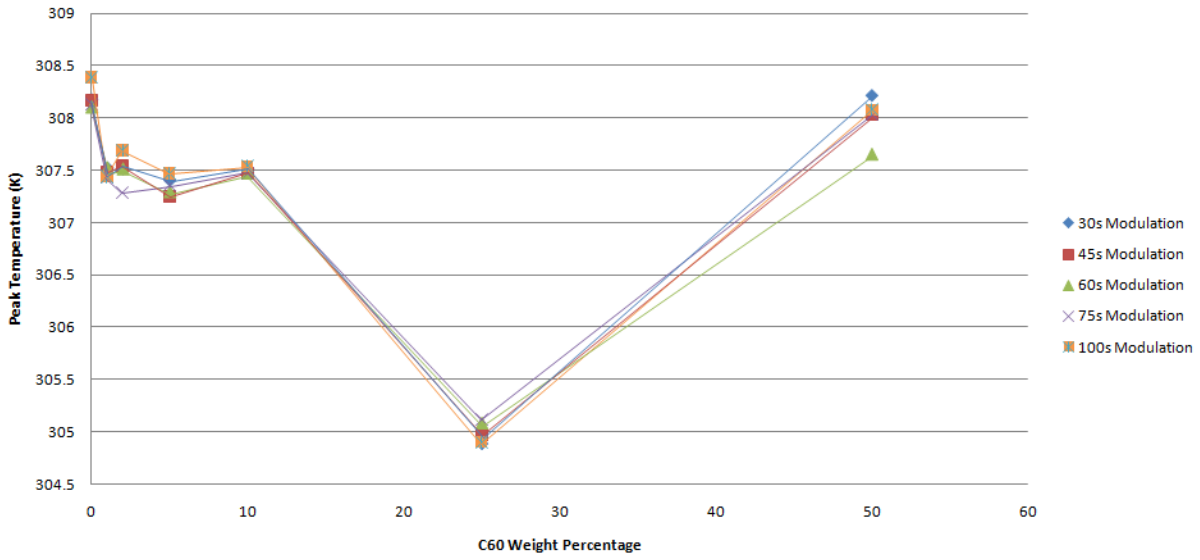

Figure 28 Peak Temperatures as a function of frequency due to temperature modulation (heat)

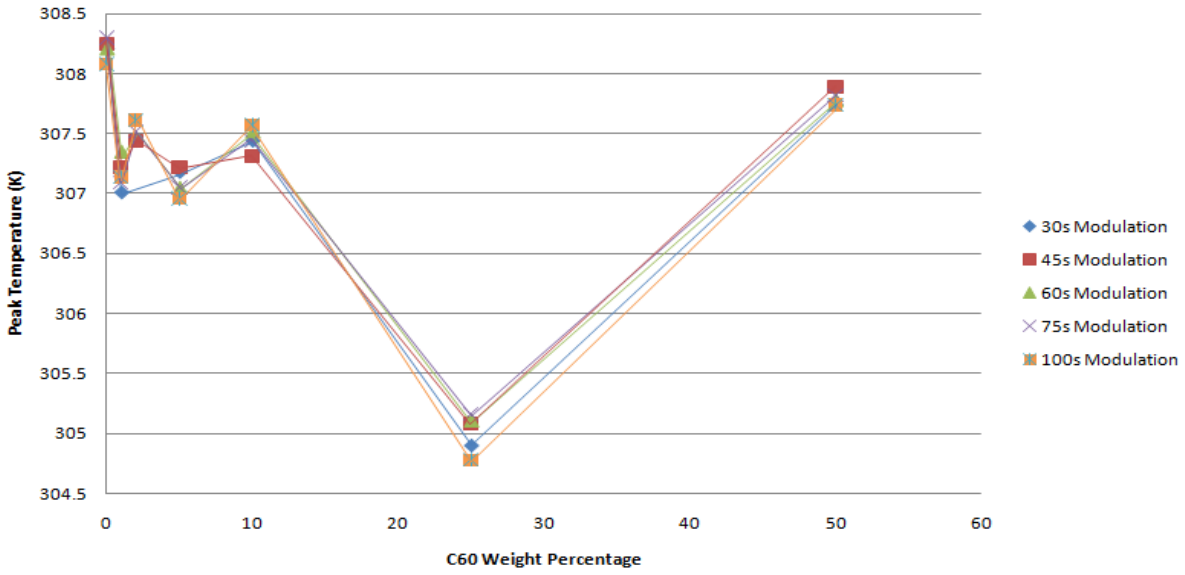

Figure 29 Peak Temperatures as a function of frequency due to temperature modulation (cool)

3.1.6 Frequency Enthalpy

The enthalpy values due to the nematic-isotropic phase transition with respect to different frequencies were different than the different scan rate measurements. The enthalpy showed some frequency dependence (the higher temperature modulation usually the higher enthalpy value), see figures 30 and 31. Also most concentrations enthalpy values were fairly close for all temperature modulations showing much less variation compared to the scan rate enthalpy comparison graph but there was still variability between modulation rates and concentrations. Again like in the scan rate enthalpy comparison the 50% concentration usually had much greater enthalpy values because its heat capacitance peaks were usually larger than the other concentrations which led to a greater area under the curve and hence a greater enthalpy. Also the 1% concentration was usually lower than all other concentrations. The heat and cools were in good agreement with one another. A table showing the actual number values represented in the enthalpy figures 30 and 31 can be found in Appendix D.

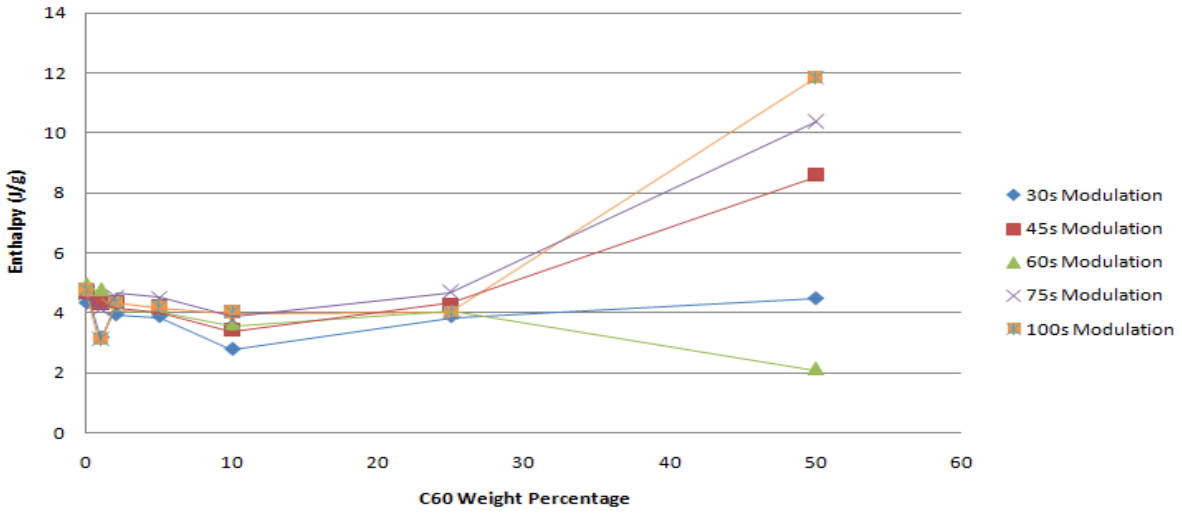

Figure 30 Enthalpy of phase transitions as a function of frequency due to temperature modulation (heat)

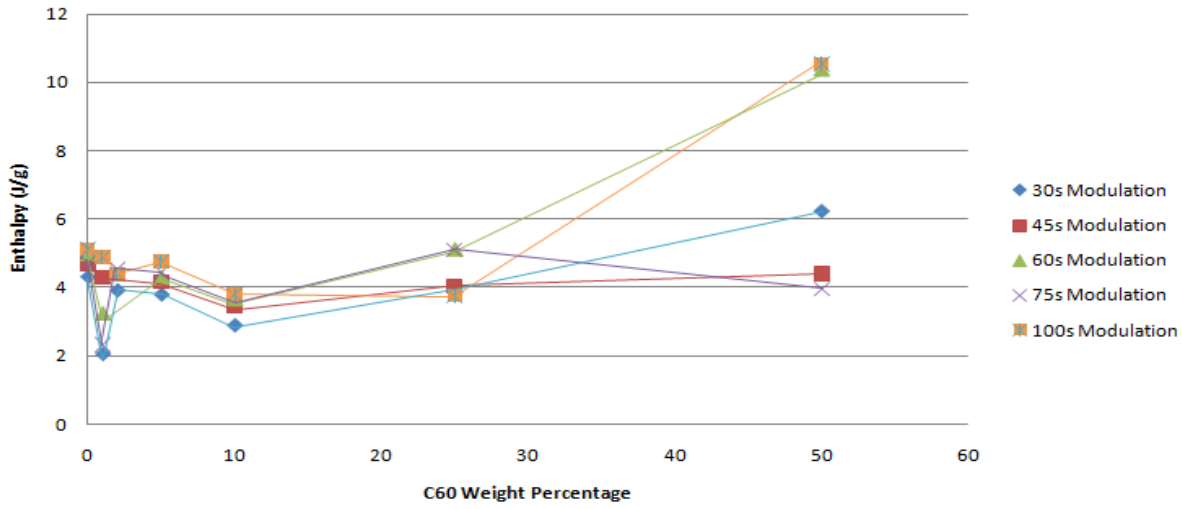

Figure 31 Enthalpy of phase transitions as a function of frequency due to temperature modulation (cool)

3.1.7 Frequency Full Width At Half Max

For different frequencies the full width at half max usually was a higher value for higher temperature modulation periods showing show frequency dependence. Like the scan rate's full width at half max the 1% concentration is consistently lower than all other concentrations. The other concentrations vary and there isn't much difference between the heat and cool see figures 32 and 33. A table showing the actual number values represented in the full width at half max figures 32 and 33 can be found in Appendix E.

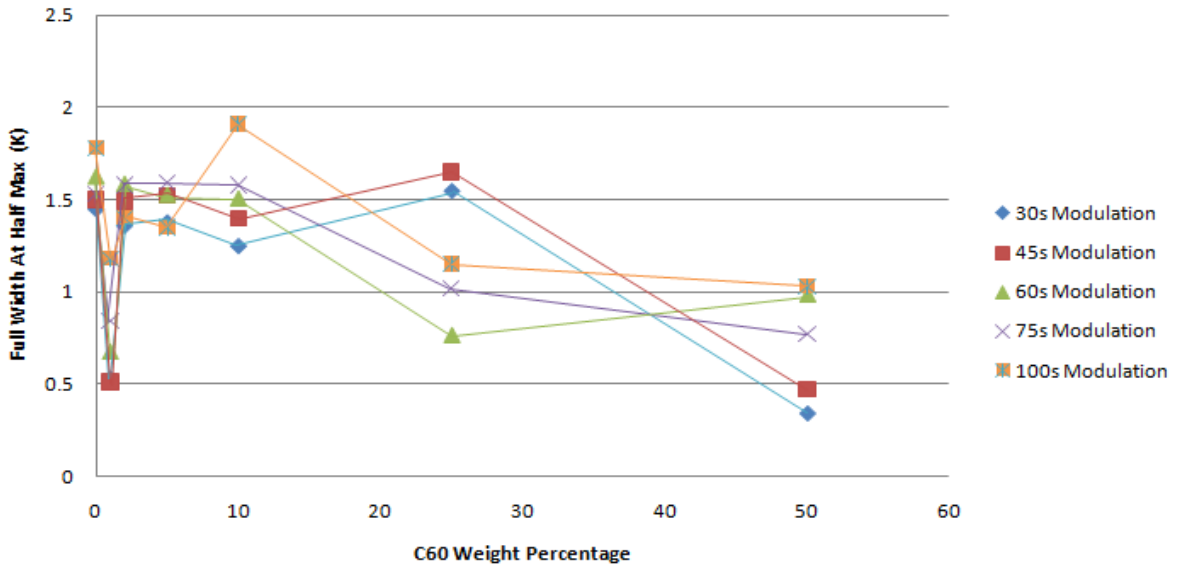

Figure 32 Full Width At Half Max of C_{60} concentration's reversible heat capacitance signal peak as a function of frequency due to temperature modulation (heat)

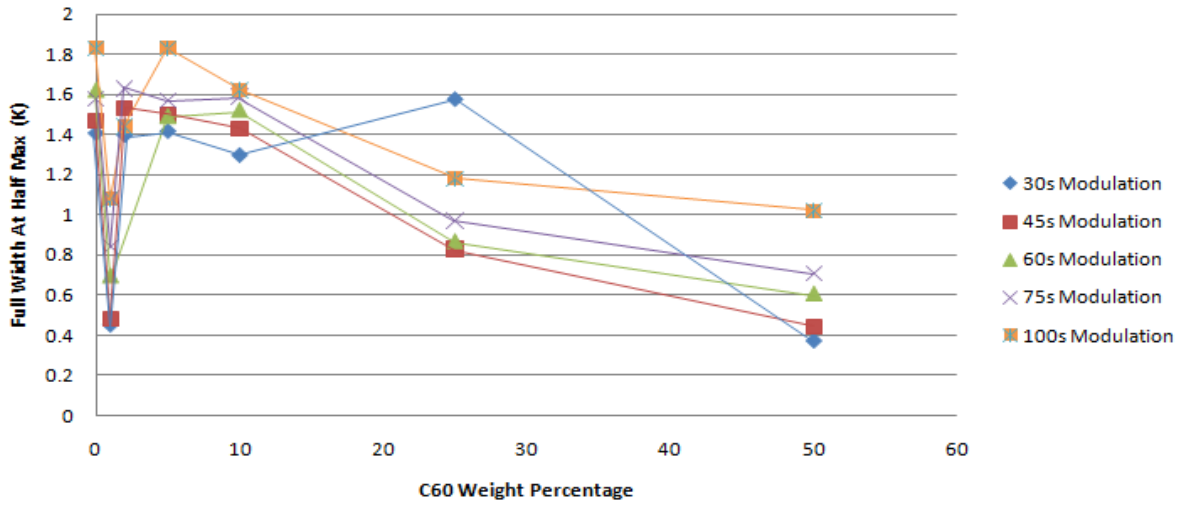

Figure 33 Full Width At Half Max of C_{60} concentration's reversible heat capacitance signal peak as a function of frequency due to temperature modulation (cool)

3.2 Microscopy results

After placing samples of 5CB with different dispersion concentrations of C_{60} into the polarized light microscope the overall structure of the molecules and pattern of C_{60} dispersion could be observed. The microscope's ocular magnification was 1.25X and the lens magnification was 10X resulting in an overall magnification of 12.5X. All microscope pictures were taken at room temperature while the liquid crystal was deep in the nematic phase. Figure 34 shows a picture of pure 5CB.

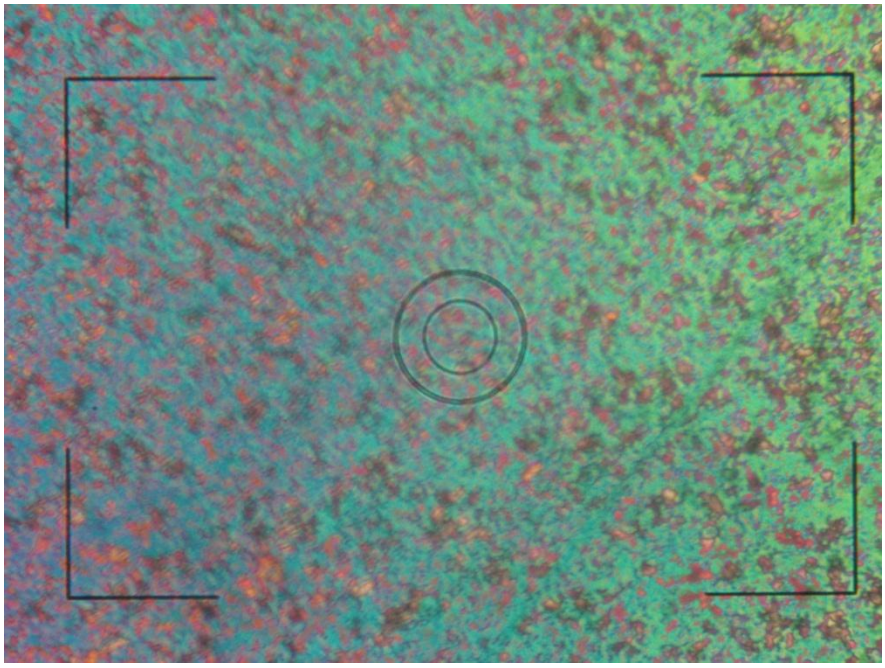

Figure 34 Pure 5CB

This picture is representative of what a typical nematic liquid crystal would look like. There are slight variations in the thicknesses of the birefringent material which cause the light wave to change phase resulting in the display of many different colors. The “thread” like defects in this image are also characteristic of 5CB in the nematic phase. A picture of the 5CB 1% C_{60} composite can be seen in figure 35.

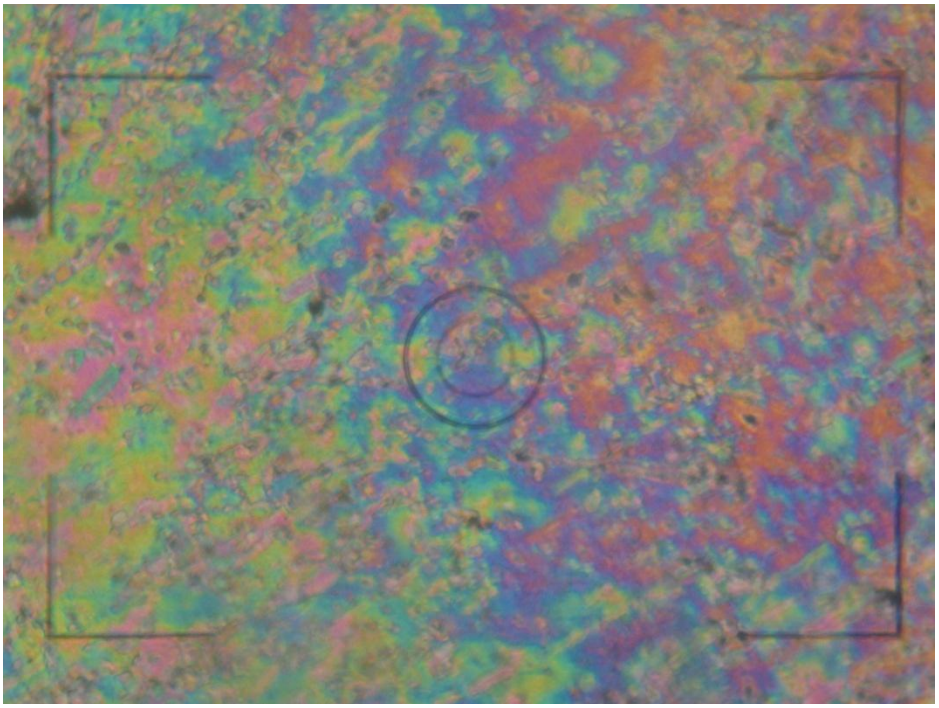

Figure 35 5CB 1% C_{60} Concentration

This image looks very similar to the pure 5CB. The C_{60} molecules seem to stick together in lumps possibly due to Van Der Waals forces. This phenomenon can be seen as the black spots due to the C_{60} molecules blocking the light from coming through. As the concentration of C_{60} increases the black spots in the image will increase. The image of the 5CB 2% C_{60} composite can be seen in figure 36. The black spots approximately double as expected.

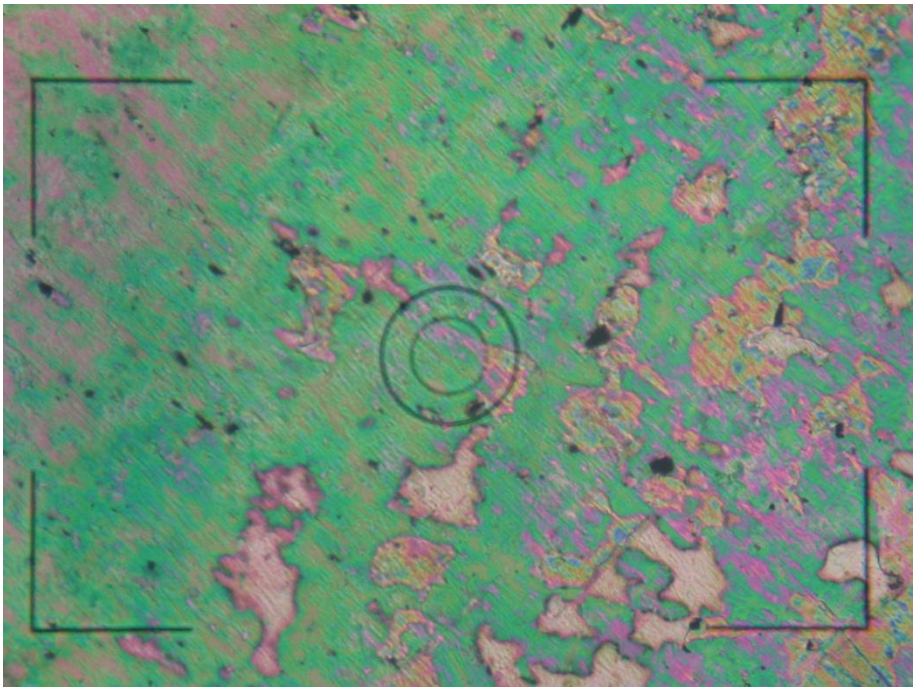

Figure 36 5CB 2% C_{60} Concentration

In the picture of the 5CB 5% C_{60} composite the visibility of the C_{60} molecules becomes easily noticeable see figure 37.

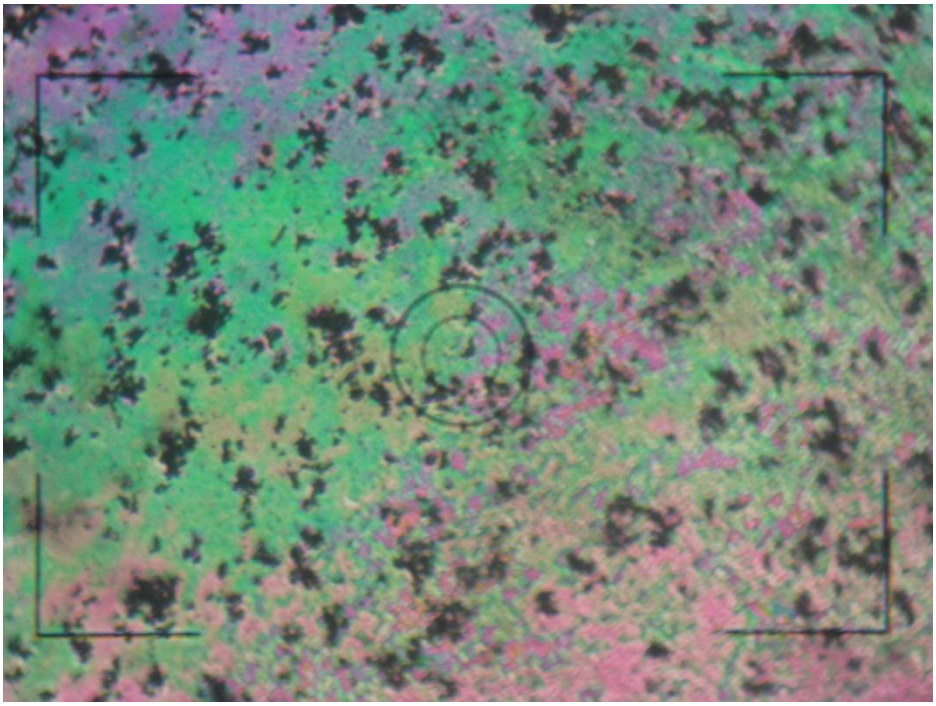

Figure 37 5CB 5% C_{60} Concentration

The 5CB 10% C_{60} concentration has double the dark spots that the 5% C_{60} concentration has. At 10% concentration the C_{60} begins to dominate the image and the spots become much larger. The C_{60} doesn't appear to be individually dispersed but is dispersed in small domains. The picture can be seen in figure 38.

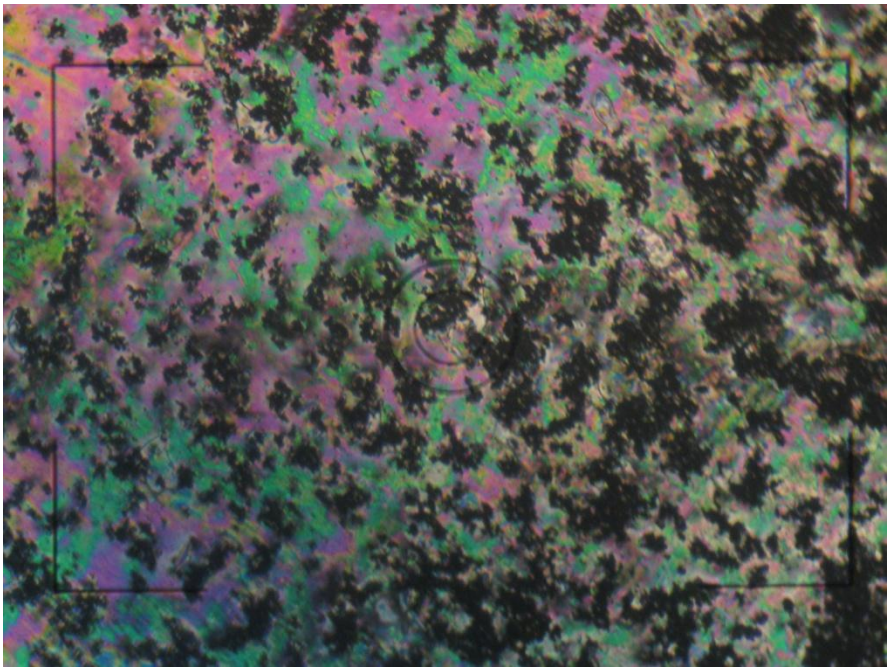

Figure 38 5CB 10% C_{60} Concentration

At 15% C_{60} concentration the small local domains appear to change from C_{60}, like in the previous concentrations, to small domains of liquid crystals. There are so many C_{60} molecules packing together the liquid crystals are forced into small pools. See figure 39.

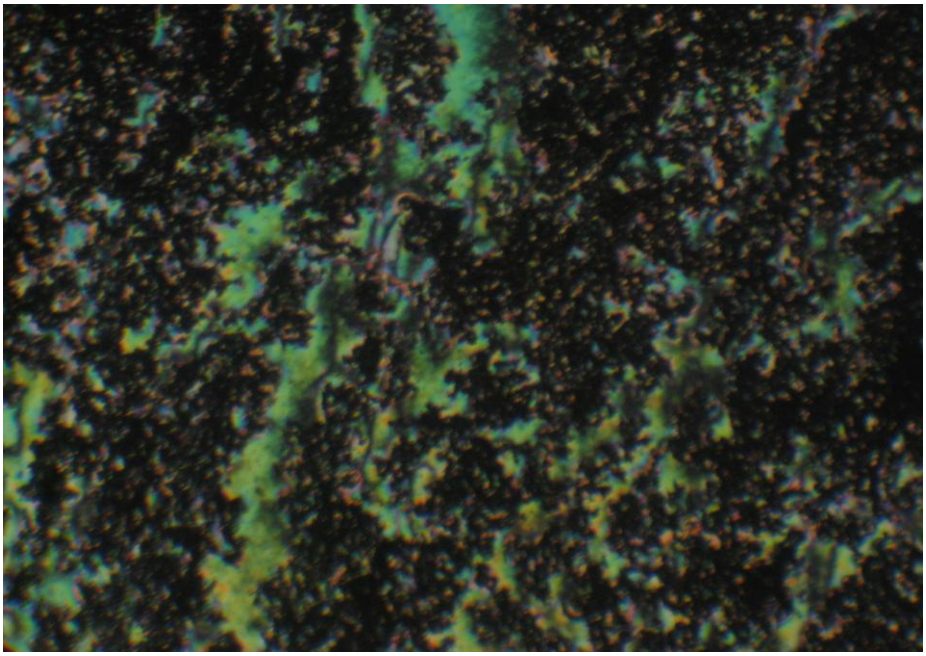

Figure 39 5CB 15% C_{60} Concentration

At 20% C_{60} weight concentration the microscope images show some interesting features. At 20% concentration, unlike all other concentration images, shows signs of multiple dispersion patterns of C_{60} 5CB molecules. In figure 40 the C_{60} formed moderately sized local domains and these domains seem pretty even dispersed in its relative local viewing area.

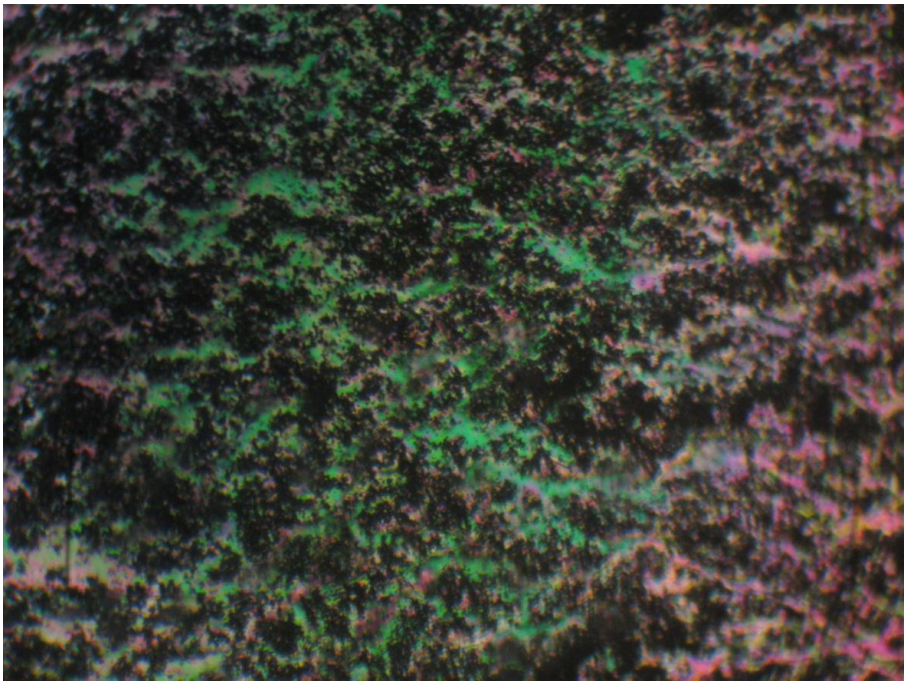

Figure 40 5CB 20% C_{60} Concentration (dispersed local domains)

However in figure 41 the image shows highly concentrated C_{60} dispersion (like will be seen in 25% concentration) with large C_{60} domains (see top left of figure 41) and large 5CB domains (see the colorful band at the bottom of figure 41). Figure 42 shows another large area where there are highly concentrated C_{60} dispersions with large C_{60} domains very similar to the images of 25% concentration.

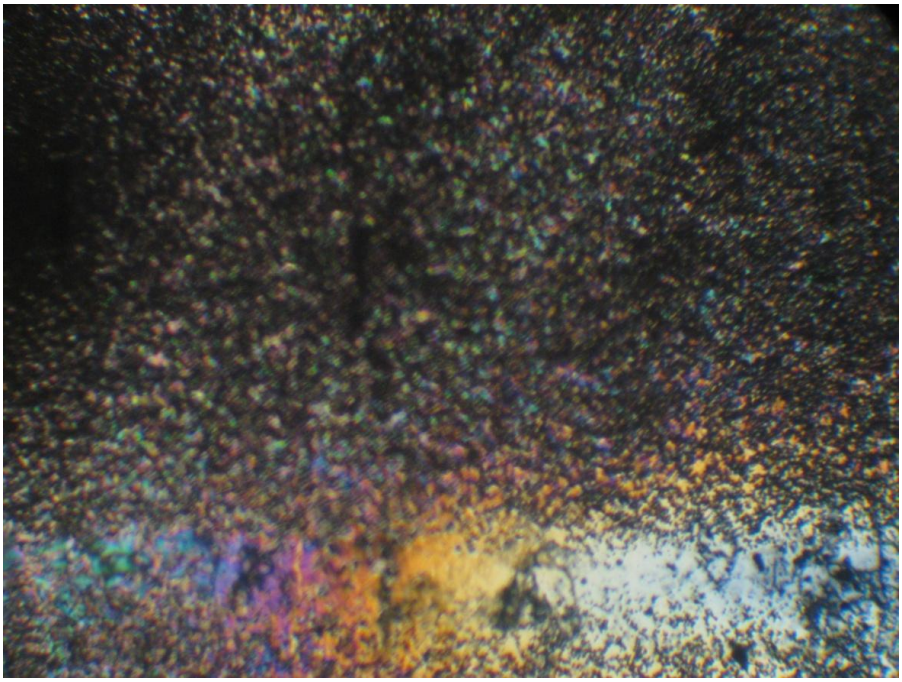

Figure 41 5CB 20% C_{60} Concentration (large local C_{60} and 5CB domains)

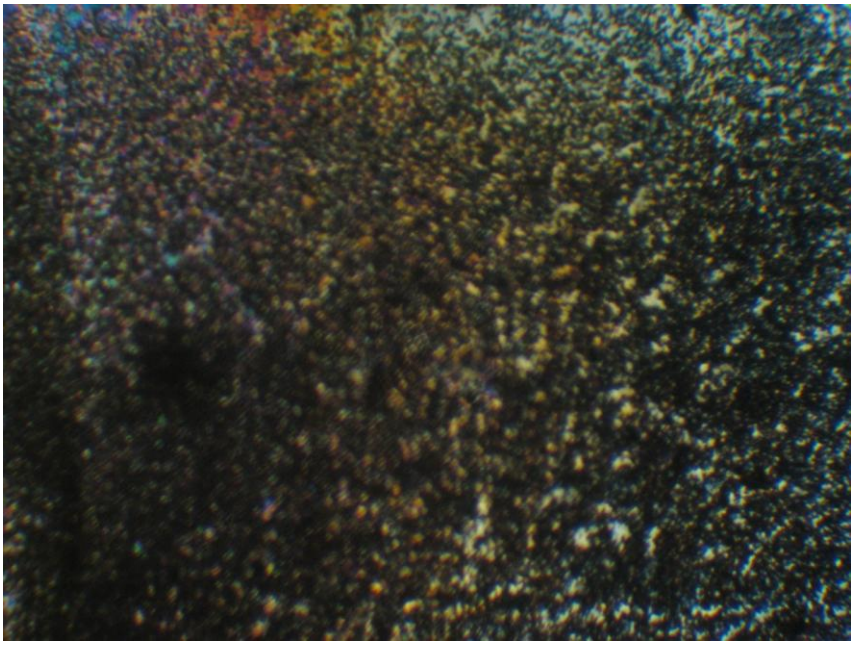

Figure 42 5CB 20% C_{60} Concentration (fairly evenly dispersed, high C_{60} concentration)

At 25% C_{60} concentration there are so many C_{60} molecules blocking the light that the image beings to look like a hubble picture the universe. Instead of patches of dark spots there are patches of colorful

liquid crystals between the cracks of the C_{60} molecules. This is considered high C_{60} concentration and the image shows apparent homogeneity. The image can be seen in figure 43.

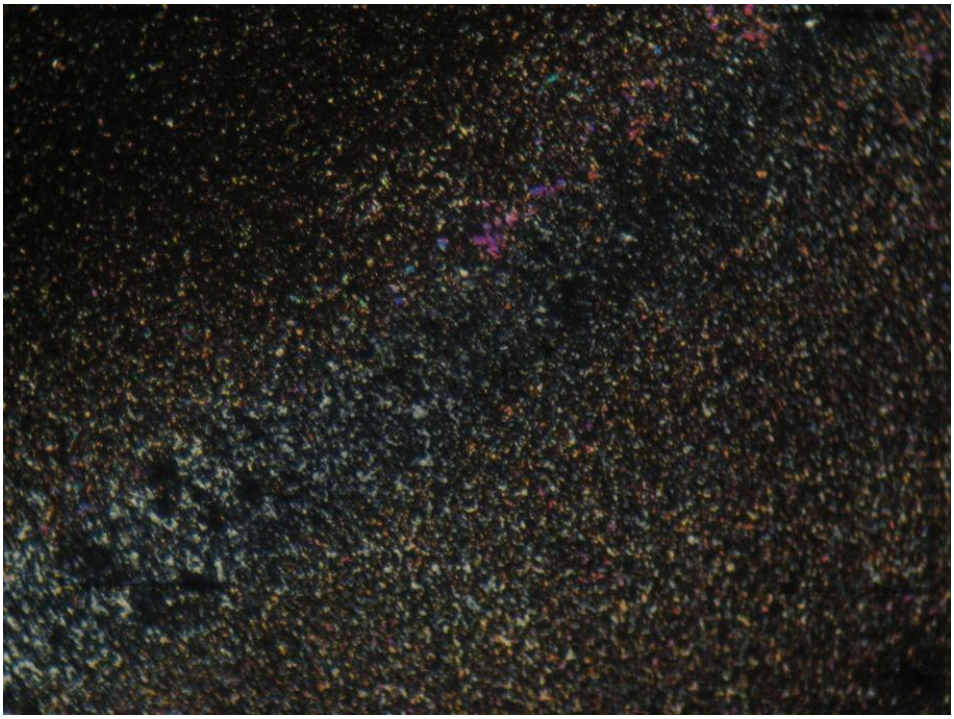

Figure 43 5CB 25% C60 Concentration

The final image was 50% concentration of C_{60}. The C_{60} completely dominates the image and is close to opaque. The 50% C_{60} composite has a very thick texture. There are a few random spots where light passes and small amounts of the 5CB can be seen, the image can be seen in figure 44.

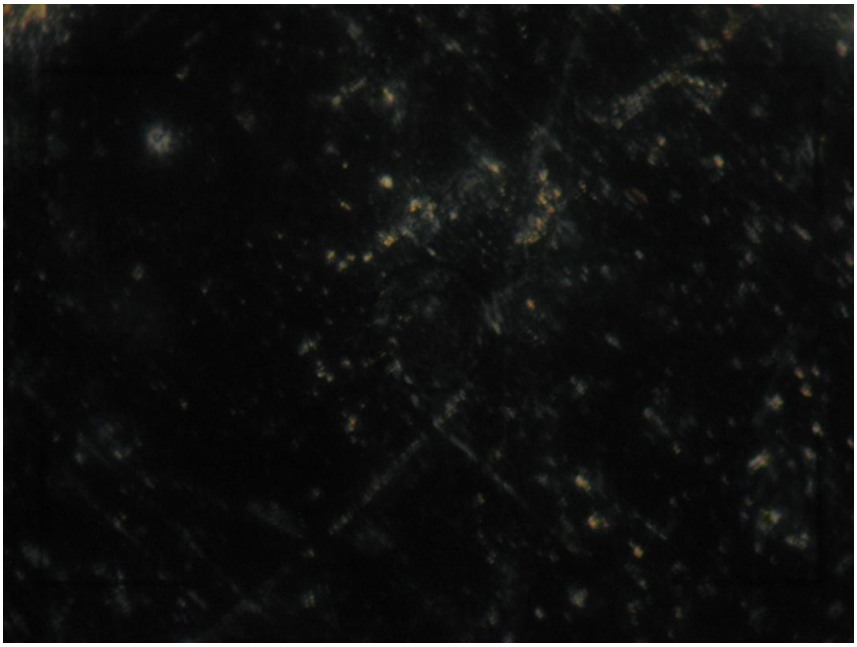

Figure 44 5CB 50% C_{60} Concentration

These pictures show how the C_{60} molecules disperse through the liquid crystal medium. The structure of this dispersion may be used as a way to resolve any unexpected phenomena that may come up during experimentation.

3.3 Steric Modeling

The steric model was designed to test whether the small domains present in the microscopic pictures could be reproduced in a macroscopic scale model of the molecules. An image of the pure 5CB model molecules can be seen in figure 65. In this model a centimeter is equivalent to a nanometer. The image shows how the molecules of 5CB align in the nematic phase with the director being along the east/west direction.

Figure 45 Model of Pure 5CB

The next model tested after the initial pure model was of the 1% C_{60} weight concentration which can be seen in figure 46. This concentration model showed the two C_{60} molecules ended up pretty close to each other after multiple mechanical disturbances. This seems consistent with the microscope pictures showing that possible that small numbers of C_{60} molecules create very small domains randomly distributed throughout the liquid crystal medium.

Figure 46 Model of 5CB with 1% C_{60} Weight Concentration

The 2% model consistently showed that the molecules would bunch together in pairs or more or just be very close in range to each other showing small local domains. This type of modeling for small concentrations like 1% and 2% is less telling because of the fact there is only a small number of C_{60} compared to a large number of 5CB molecules, and for only using 500 model 5CB molecules only a small window of the structure can be seen and with only 2 or four C_{60} molecules for the model it's hard to see an over domain effect or to see grouping of C_{60} at all. Even though the model C_{60} molecules fairly consistently ended up around each other the model would have been more effective with a larger number of model molecules, for larger concentrations 500 model liquid crystal molecules is sufficient.

Figure 47 Model of 5CB with 2% C_{60} Weight Concentration

The 5% modeling appears to be in agreement with the microscopic pictures. Multiple small domains are beginning to form and the domains are becoming bigger in size, see figure 48.

Figure 48 Model of 5CB with 5% C60 Weight Concentration

The models representing 10% and 15%, in figures 49 and 50, show the general trend seen in microscopic pictures. The domains continue to grow larger and more frequent. Most of the model C_{60} molecules gather around each other and it is random to find one by itself in its own local area.

Figure 49 Model of 5CB with 10% C60 Weight Concentration

Figure 50 Model of 5CB with 15% C60 Weight Concentration

The 20% model seen in figure 51 begins to show the dominance of the C_{60} domains. The domains are increasingly larger and extent well into the layers of model molecules.

Figure 51 Model of 5CB with 20% C60 Weight Concentration

The 25% model shows large domains of C_{60} grouping together, see figure 52. At first glance the image doesn't appear to show the highly concentration dispersion that the microscope images show however, what is not shown in the model images is when goings through the layers of the C_{60} these large concentrated dispersions are present. If light was coming from the bottom like in a microscope the C_{60} molecules at the lower layers would have blocked the light from coming through giving the highly concentrated appearance but the images only shows the top layer.

Figure 52 Model of 5CB with 25% C_{60} Weight Concentration

The 50% model seems to be in good agreement with the microscopic images. The model is completely domainated by the C_{60} molecules and they appear to form one huge domain with random 5CB domains dispersed throughout. The 50% model image can be seen in figure 53.

Figure 53 Model of 5CB with 50% C_{60} Weight Concentration

4. Conclusion

In conclusion, the MDSC heat capacitance signals showed that as the concentration of C_{60} becomes greater the 5CB nematic to isotropic phase transition occurs at lower temperatures compared to the pure 5CB overall. This seems to be an overall reoccurring trend in all scan rate experimentation and frequency experimentation. Although with percentages between 1% and 10% the values are all very close and they do experience a phase transition a temperature less than the bulk 5CB, the overall trend cannot be observed. The closeness of these values could be due to small amounts of error in the sampling or cell making process. Concentrations of 15% and 20% were tested with a scan rate dependence to see if a trend could be observed of a declining peak temperature reaching a minimum at 25%. However these two concentrations yielded varying results similar to what the 50% concentration shows. In all scans the 25% concentration always had the lowest transition temperature and didn't fluctuate much which is most likely due to the composites overall homogeneity and dispersion of C_{60} with in the 5CB medium. The 50% C_{60} sample is so over saturated with the C_{60} that only small domains filled with 5CB contribute to the phase transition readings which yield result close to those of the pure 5CB or very random results. This local domain phenomena may also to causing be occurring at smaller C_{60} concentrations but with C_{60} trapped in local domains. The enthalpy and full width at half max show that some of the values fluctuate which may be due to small domains filled with C_{60} molecules and these "lumps" of C_{60} are dispersed throughout the liquid crystal medium and experience Brownian motion due to the 5CB molecules impacting the lumps from all directions. The evidence of these C_{60} lumps and their growth as concentrations become larger is found in the microscopic images. Further evidence supporting the notion of isolated molecular domains comes from steric packing model. This macroscopic model shows how these rod like shapes relative to different amounts of roughly spherical C_{60}. These steric experiments show that indeed, after repeated mechanical disturbance and quenching, as the

concentrations of C_{60} becomes larger so does the size, number, and complexity of the domains created by the C_{60} molecules packing together. These findings show that odd MDSC results may be due to the geometries of 5CB and C_{60} and how different concentrations minimize space and energy by fitting into domain structures.

There are many ways to study these 5CB fullerene composites more closely in the future. One could see whether some of the randomness of the values could be due to a cyclical process. There more times the sample is heated or cooled could affected the results of the experimentation. An improvement not taken advantage of in this project could have been performing all experimentation continuously because the experiments performed in this project were discontinuous, samples tested during winter months would exhibit a melting transition during the samples first heat of these day because of the ambient temperature. This solid to nematic transition may or may not have had some effect on some of the results. To gain further insight into this project one may want to look at all concentrations that were not tested in this project. One may use a different thermal technique on this composite such as AC calorimetry or even traditional DSC. One may also want to look more into the steric nature of the phenomena surrounding this composite. One could create a computer program representing the steric modeling and run a simulation. One could do a statistical analysis of the steric model or microscopic images using software which can convert images into a brightness factor and this factor could act as an "order parameter" and give a quantitative analysis of the composites ordering. One may also want to repeat the steric experiments in a way that the same amount of mechanical agitation is used for each concentration and ensure that the mechanical agitation is consistent and not too strong or too weak. Also one could perform any these experiments with a larger or smaller fullerene such as C_{20} or C_{70} or one may use an entirely different fullerene shape or another nanoparticle all together or one may even use a different liquid crystal such as 8CB and look at how the different geometries of the molecules affect their properties. One could also probe deeper in the molecular

packing by using stronger imaging device like a scanning electron microscope or some other scattering technique. One could look at other properties of the composite such as its optical properties like the composites overall index of refraction or other properties such as its dielectric constant.

Works Cited

1. Denker, John. "The Laws of Thermodynamics." 2010. http://www.av8n.com/physics/thermo-laws.htm.

2. Liquid Crystal Group. "What are liquid crystals?" *Liquid Crystal Group: Chalmers University of Technology Department of Microtechnology and Nanoscience.* February 12, 1998. http://www.mc2.chalmers.se/mc2/pl/lc/engelska/frame.html.

3. Khoo, Iam-Choon. *Liquid Crystal Physical Properties and Nonlinear Optical Phenomena.* Singapore: John Wiley & Sons, Inc., 1995.

4. Rapid Intelligence. "StateMaster- Encyclopedia: Phase Transitions." *StateMaster.* http://www.statemaster.com/encyclopedia/Phase-transition.

5. Oxford University. "History of Liquid Crystals." *Liquid Crystal Technology Homepage.* http://www.eng.ox.ac.uk/lc/introduction/history_1.html (accessed 2009).

6. Slucklin, Timothy J., David A. Dunmur, and Horst Stegemeyer. "Crystals that Flow: Classic papers from the history of liquid crystals." *History of Liquid Crystals Homepage.* Taylor and Francis. 2004. http://www.personal.soton.ac.uk/tim/crystals_that_flow/homepage.htm.

7. Case Western Reserve University. "Virtual Textbook." *Polymers & Liquid Crystals.* 2004. http://plc.cwru.edu/tutorial/enhanced/files/textbook.htm.

8. The Nobel Foundation. "Liquid crystals." *NobelPrize.org.* September 9, 2003. http://nobelprize.org/educational_games/physics/liquid_crystals/history/.

9. Saeva, Franklin D. *Liquid Crystals The Fourth Sate of Matter.* New York: Marcel Dekker, Inc., 1979.

10. Gilles de Gennes, Pierre. *Physics of Liquid Crystals.* New York: Oxford University Press, 1974.

11. Department of Materials Science and Metallurgy. "Order and disorder – molecular orientation." *University of Cambridge.* http://www.doitpoms.ac.uk/tlplib/liquid_crystals/order_disorder_orientation.php.

12. Barrett Research Group. "Introduction to Liquid Crystals." *McGill University Department of Chemistry.* http://barrett-group.mcgill.ca/teaching/liquid_crystal/LC02.htm.

13. Stille. "3D representation of a liquid crystal in the isotropic state." *Wikimedia Commons.* May 31, 2008. http://commons.wikimedia.org/wiki/File:Isotropic3d.png.

14. Khoo, I. C., and S. T. Wu. *Optics and Nonlinear Optics of Liquid Crystals.* Singapore: World Scientific, 1992.

15. Oxford University. "Smectics." *Liquid Crystal Technology Homepage.* http://www.eng.ox.ac.uk/lc/introduction/smectics_1.html (accessed 2009).

16. Winter, Mark. "Carbon Allotrope Information." *WebElements Periodic Table of Elements.* http://www.webelements.com/carbon/allotropes.html.

17. Chandrasekhar, S. *Liquid Crystals.* 2nd Edition. New York: Cambridge University Press, 1992.

18. Case Western Reserve University. "Virtual Textbook." *Chemical Properties of Liquid Crystals.* 2004. http://plc.cwru.edu/tutorial/enhanced/FILES/lc/chem/chem.htm.

19. Buka, Agnes, and Lorenz Kramer. *Partially Ordered Systems: Pattern Formation in Liquid Crystals.* New York: Springer-Verlag New York, Inc., 1996.

20. AZoNano. "BuckyBalls - A Nanotechnology Building Block, How To Make Them, History, Properties and Applications." *The A to Z of Nanotechnology- Journal of Nanotechnology Online.* November 8, 2006. http://www.azonano.com/Details.asp?ArticleID=1781.

21. 7th Wave, Inc. "Nanotubes and Buckyballs." *Nanotechnology Now.* June 27, 2009. http://www.nanotech-now.com/nanotube-buckyball-sites.htm.

22. Eftekhari, Ali. "What is Nano? Scientific Facts About Nanotechnology & Nanoscience." *suite101 Insightful Writers. Informed Readers.* http://inderdisciplinaryscience.suite101.com/article.cfm/nano.

23. Stringer, Tish. "Buckyballs: Their history and discovery." *Connexions.* February 20, 2007. http://cnx.org/content/m14355/latest/.

24. Northwestern University. "NSF Summer Institute on Nanomechanics, Nanomaterials and Micro/Nanomanufacturing." *Northwestern University.* 2007. http://www.tam.northwestern.edu/summerinstitute/_links/course1-2009.htm.

25. Segawa, Craig. "The Buckyball." *Honolulu Community College.* http://www.insite.com.br/rodrigo/bucky/buckyball.txt.

26. SES Research. "Physical Properties of Fullerenes." *SES Research.* 2007. http://sesres.com/PhysicalProperties.asp.

27. Sigdel, Krishna P., and Rajratan Basu. "Isotropic to Nematic Phase Transition in Carbon Nanotube dispersed Liquid Crystal." *arXiv.* January 6, 2010. http://aps.arxiv.org/PS_cache/arxiv/pdf/0905/0905.2779v1.pdf.

28. TA Instruments."DSC Power Point." *TA Instruments Thermal Analysis Introduction.*

29. TA Instruments. "MDSC Quickstart." *MDSC e-Training course.* http://www.tainstruments.com/main.aspx?id=129&n=3&siteid=11.

30. Thomas, Leonard C. *MDSC Paper #2 Modulated DSC Basics; Calculation and Calibration of MDSC Signals.* New Castle: TA Instruments, 2005.

31. Thomas, Leonard C. *MDSC Paper #1 Why Modulated DSC? An Overview and Summary of Advantages and Disadvantages Relative to Traditional DSC.* New Castle: TA Instruments, 2005.

32. Thomas, Leonard C. *MDSC Paper #9 Measurement of Accurate Heat Capacity Values.* New Castle: TA Instruments, 2005.

33. TA Instruments. *Purge Gas Recommendations for use in Modulated DSC.* Thermal Analysis & Rheology, New Castle: TA Instruments.

34. TA Instruments. "DSC Brochure." *TA Instruments Thermal Analysis.*

35. Thomas, Leonard C. *MDSC Paper #4 Advanced TZero MDSC; Calculation of MDSC Signals, Including Phase Lag Correction.* New CAstle: TA Instruments, 2005.

36. Robinson, Philip C., and Michael W. Davidson. "Introduction to Polarized Light Microscopy." *Nikon MicroscopeU The Sourse for Microscopy Education.*
http://www.microscopyu.com/articles/polarized/polarizedintro.html.

37. Case Western Reserve University. "Virtual Textbook." *Light and Polarization.* 2004.
http://plc.cwru.edu/tutorial/enhanced/files/lc/light/light.htm.

38. Case Western Reserve University. "Virtual Textbook." *Birefringence in Liquid Crystals.* 2004.
http://plc.cwru.edu/tutorial/enhanced/files/lc/biref/biref.htm.

Appendix

A. Scan Rate

1 K/min

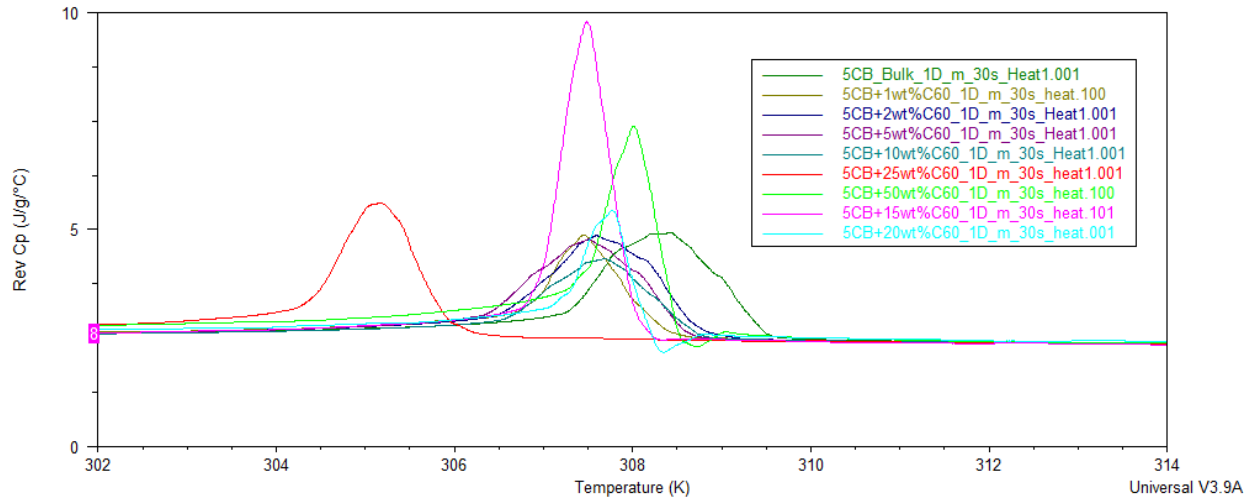

Figure 54 Reversible Cp 1 K/min (heat)

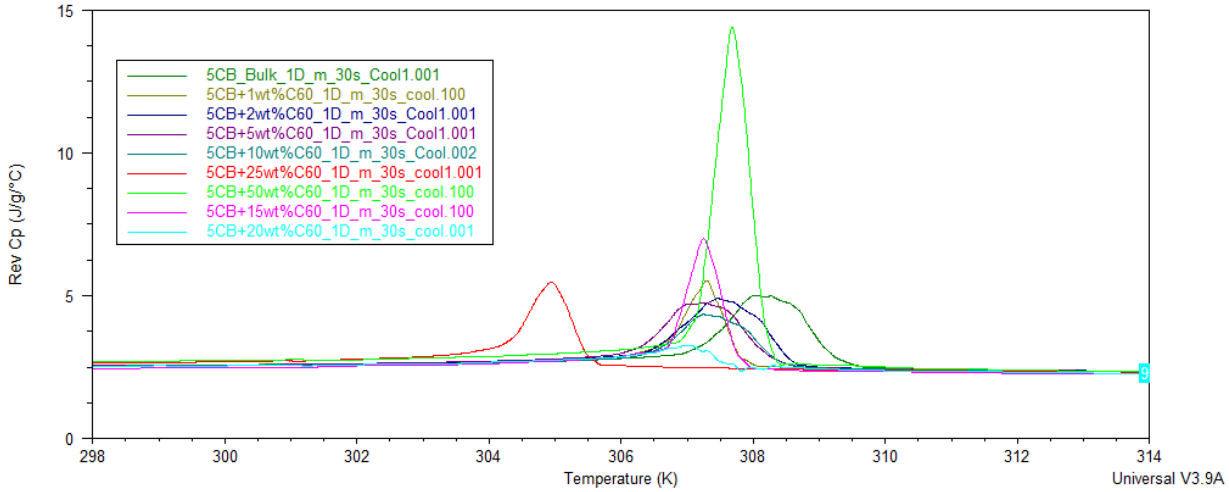

Figure 55 Reversible Cp 1 K/min (cool)

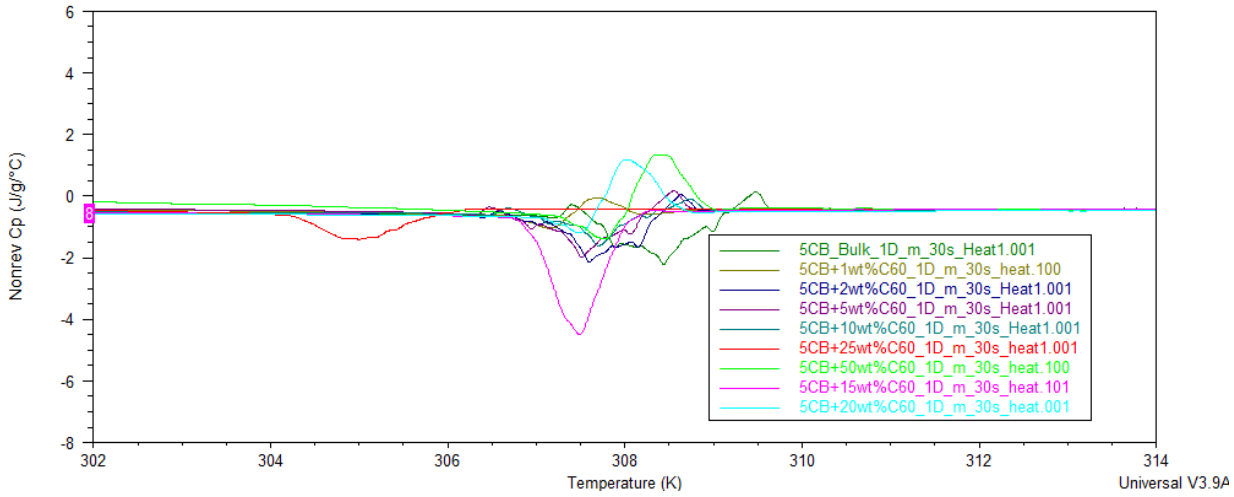

Figure 56 Nonreversible Cp 1 K/min (heat)

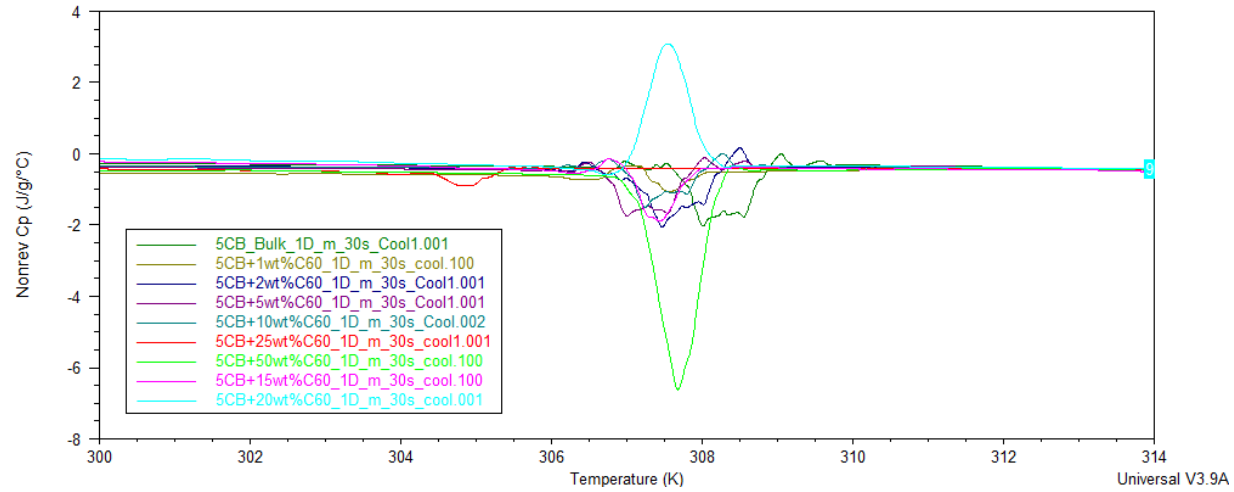

Figure 57 Nonreversible Cp 1 K/min (cool)

2 K/min

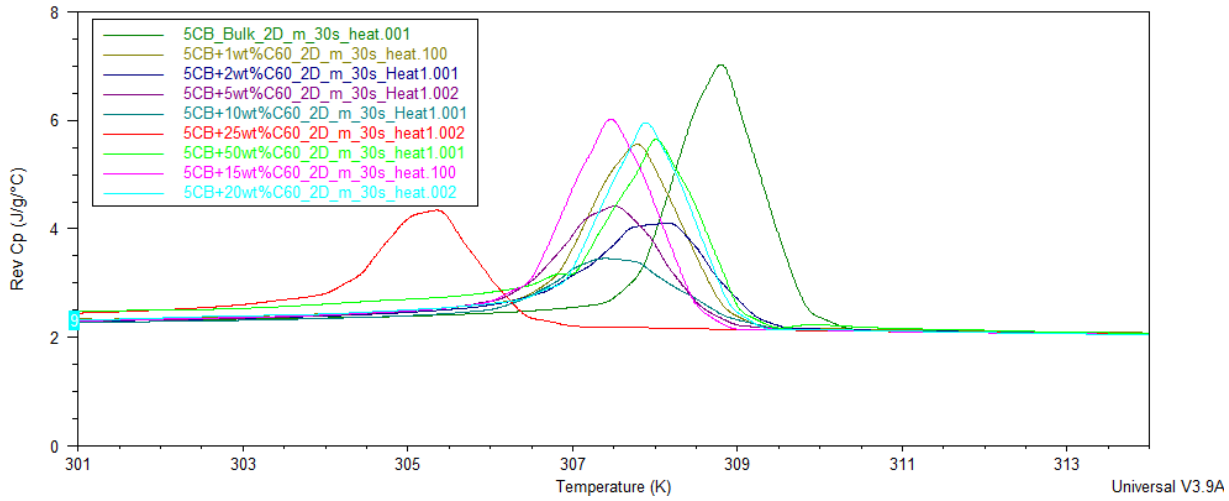

Figure 58 Reversible Cp 2 K/min (heat)

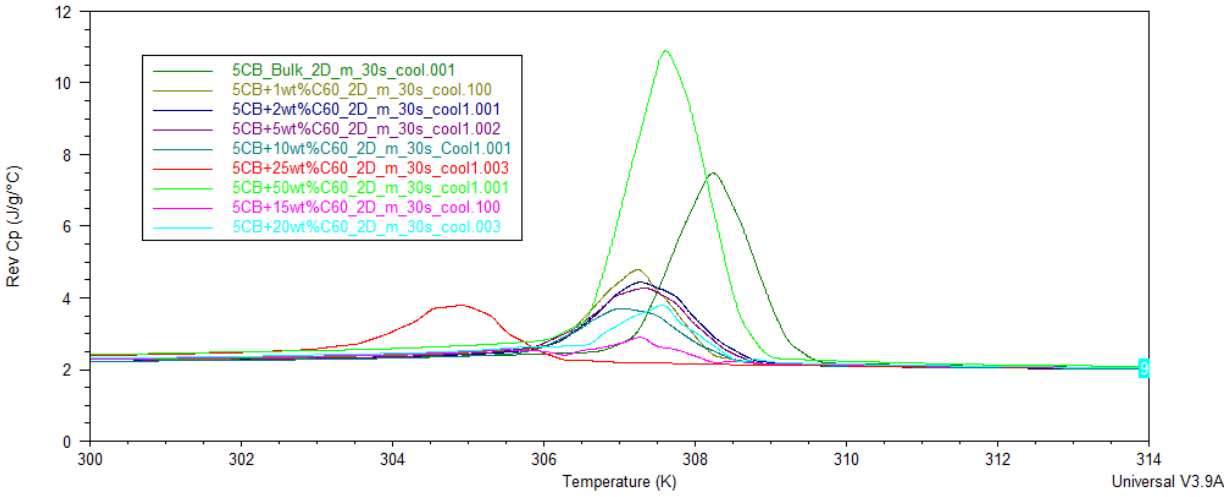

Figure 59 Reversible Cp 2 K/min (cool)

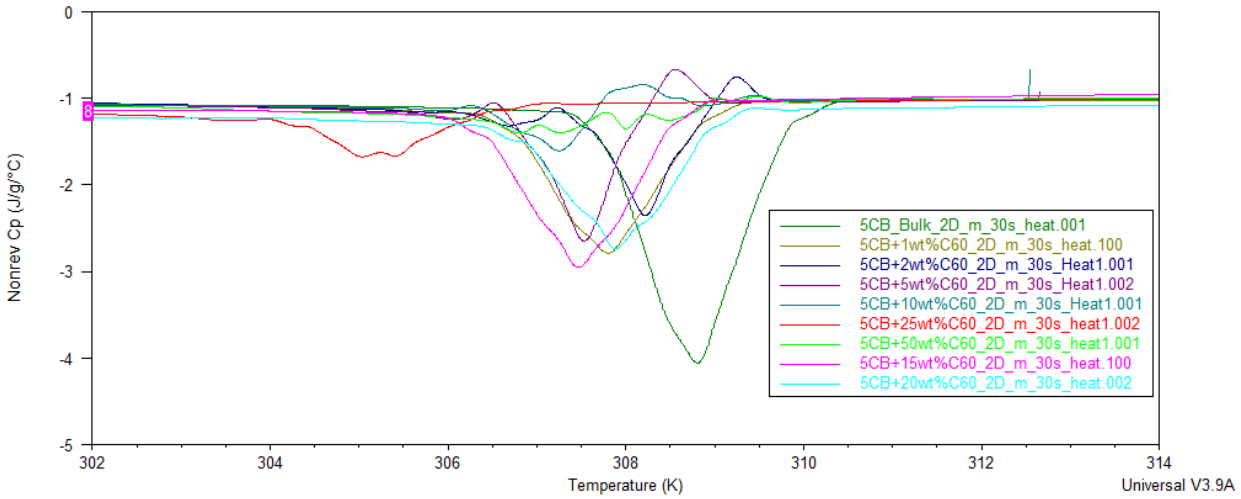

Figure 60 Nonreversible Cp 2 K/min (heat)

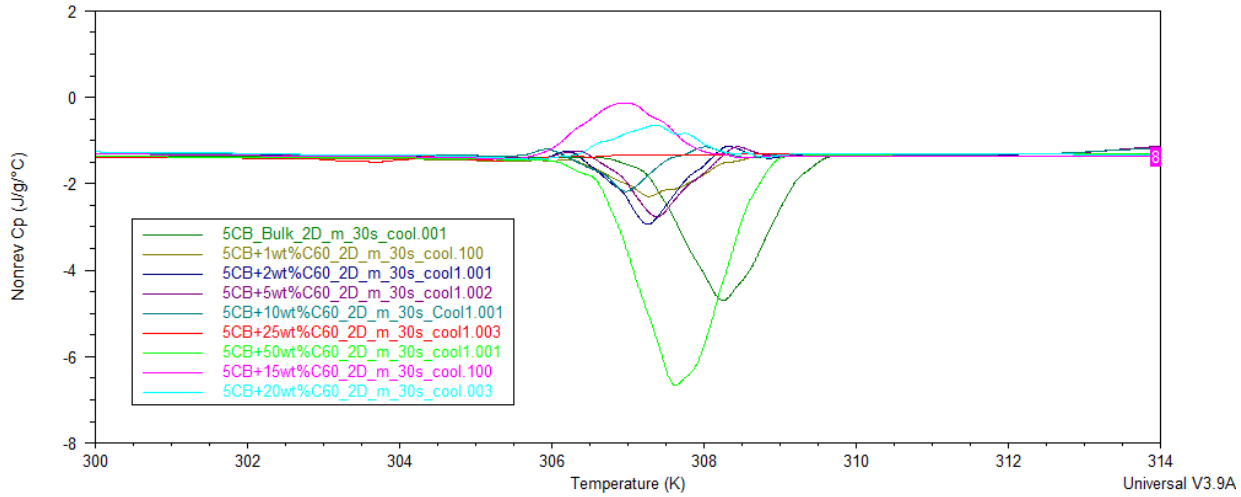

Figure 61 Nonreversible Cp 2 K/min (cool)

3 K/min

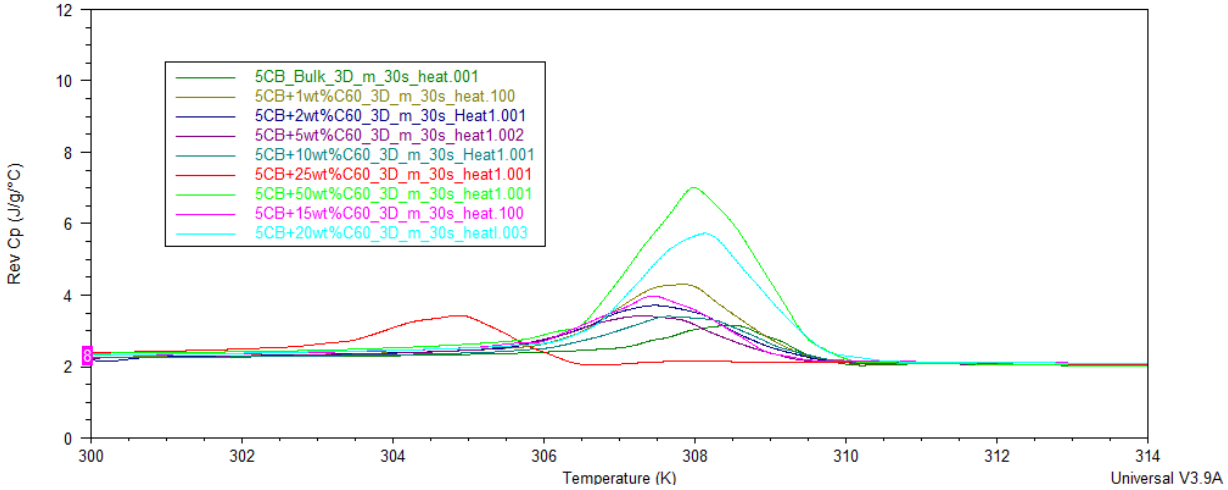

Figure 62 Reversible Cp 3 K/min (heat)

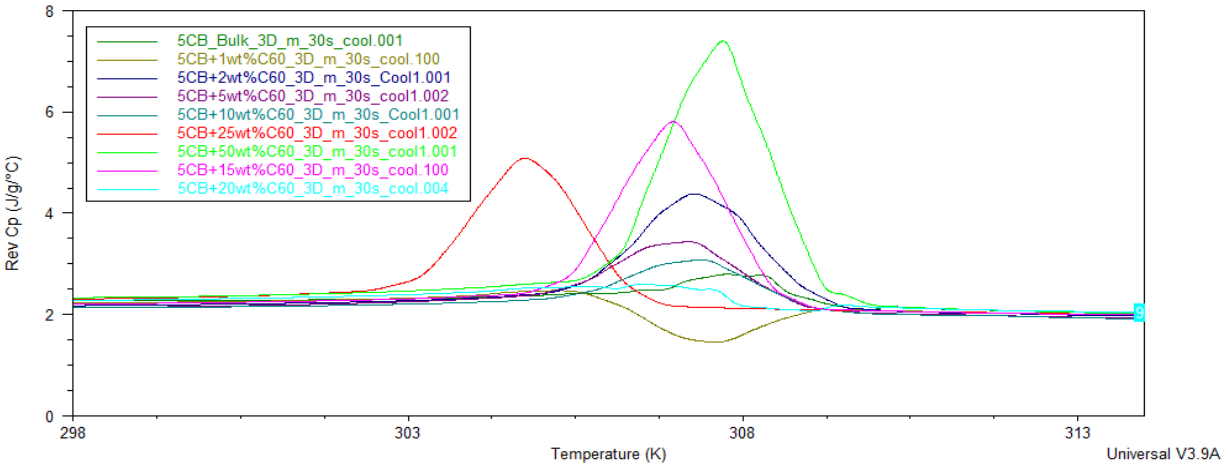

Figure 63 Reversible Cp 3 K/min (cool)

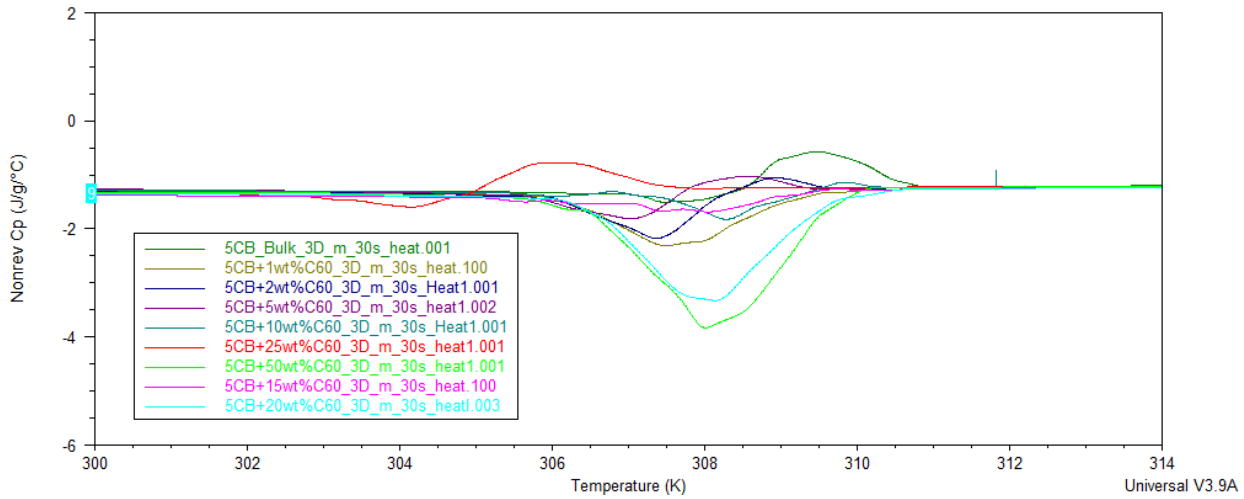

Figure 64 Nonreversible Cp 3 K/min (heat)

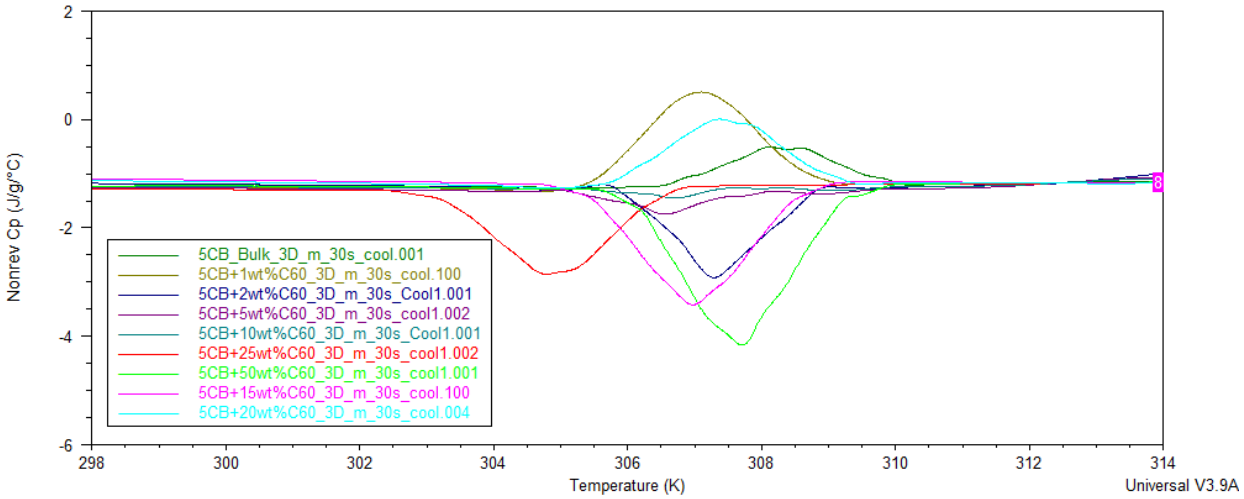

Figure 65 Nonreversible Cp 3 K/min (cool)

B. Temperature Modulation

45s Temperature Modulation

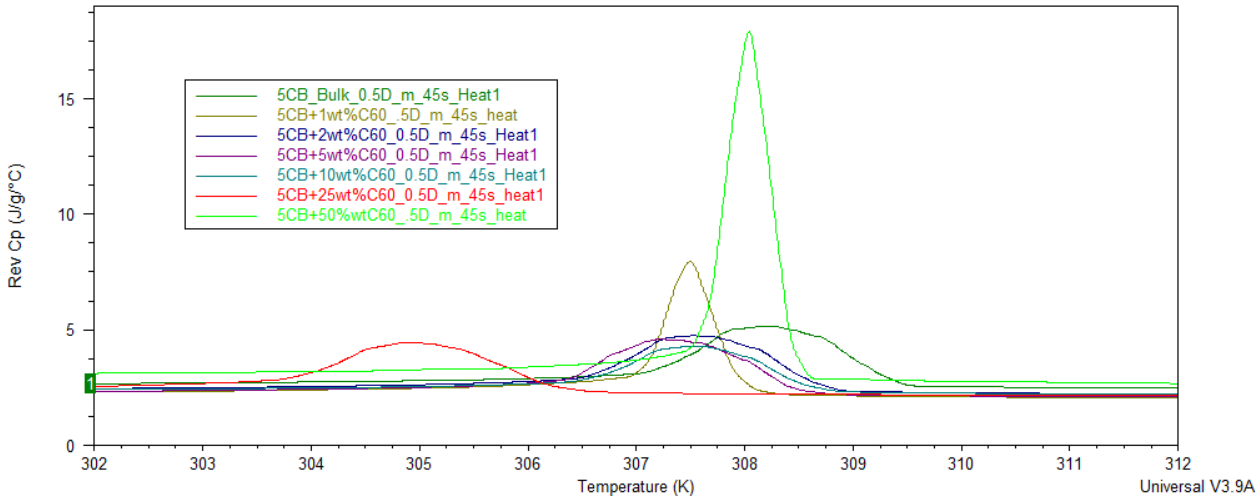

Figure 66 Reversible Cp 45s Modulation (heat)

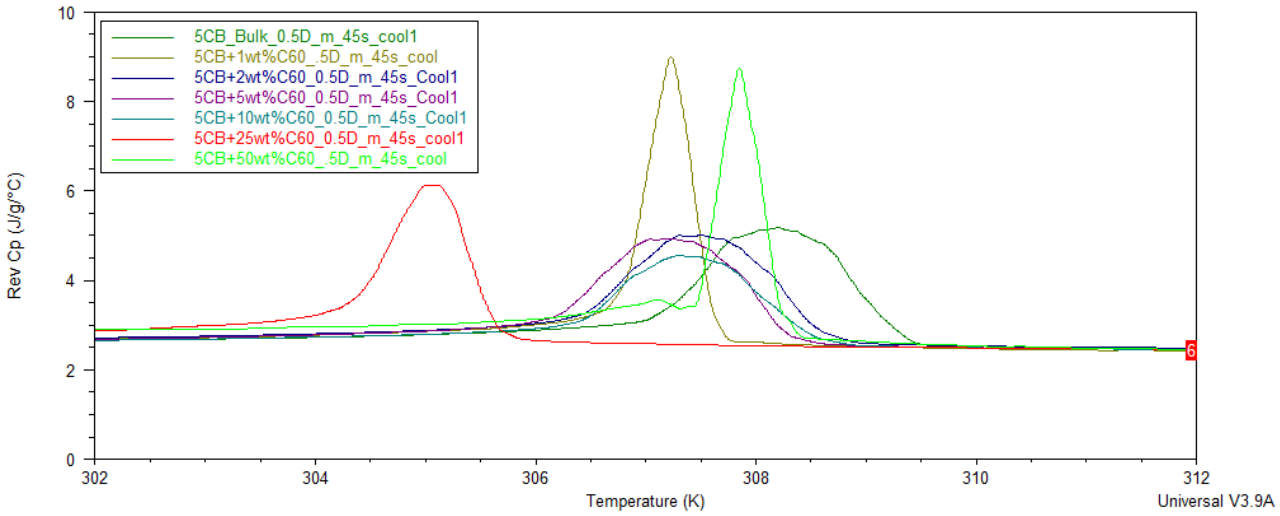

Figure 67 Reversible Cp 45s Modulation (cool)

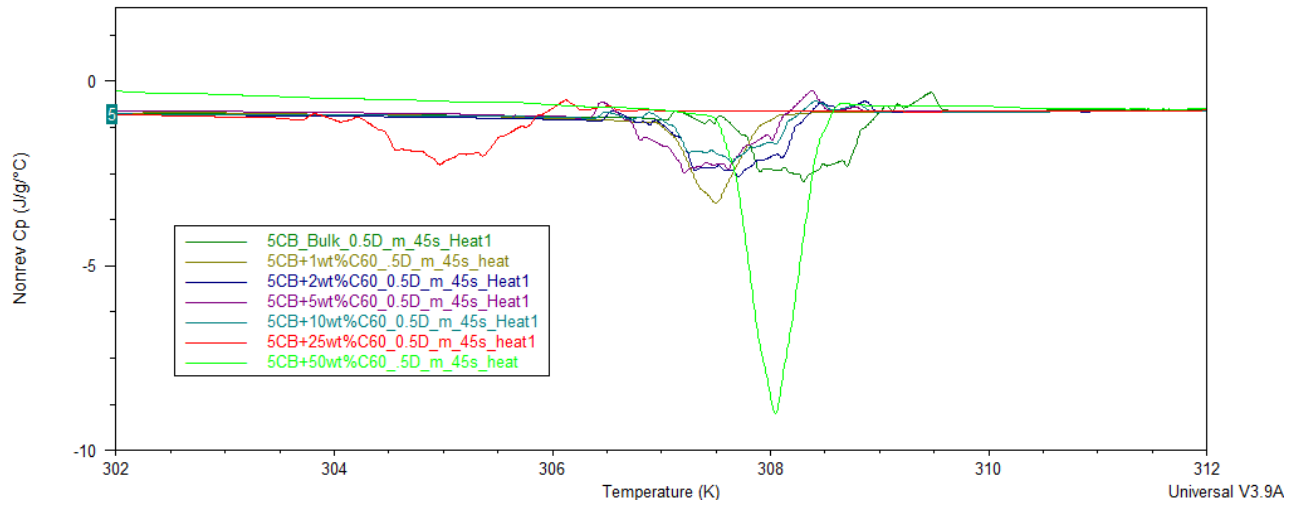

Figure 68 Nonreversible Cp 45s Modulation (heat)

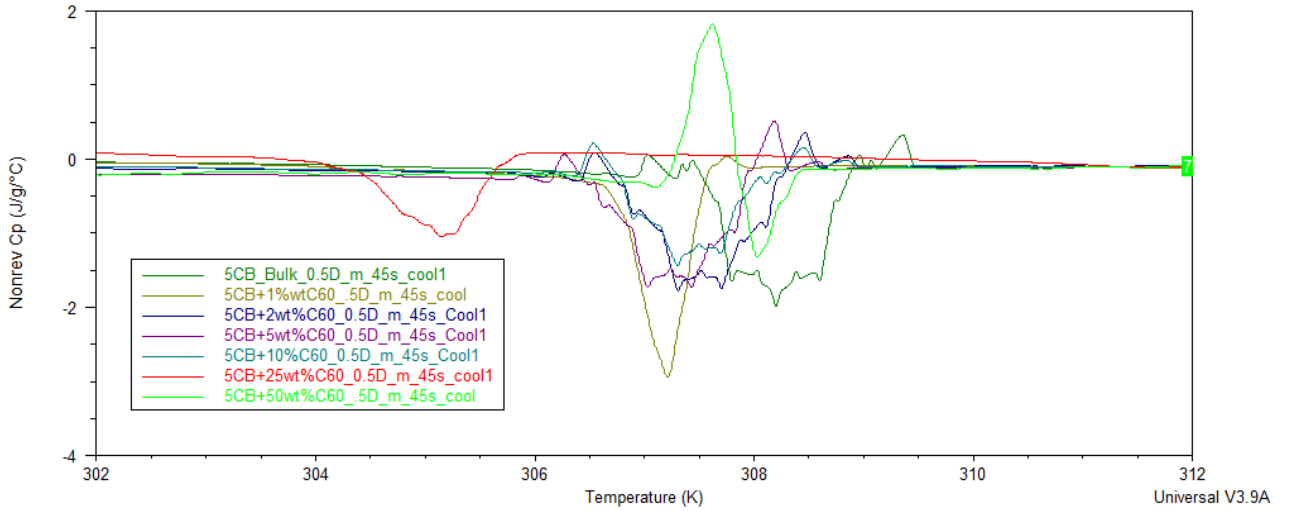

Figure 69 Nonreversible Cp 45s Modulation (cool)

60s Temperature Modulation

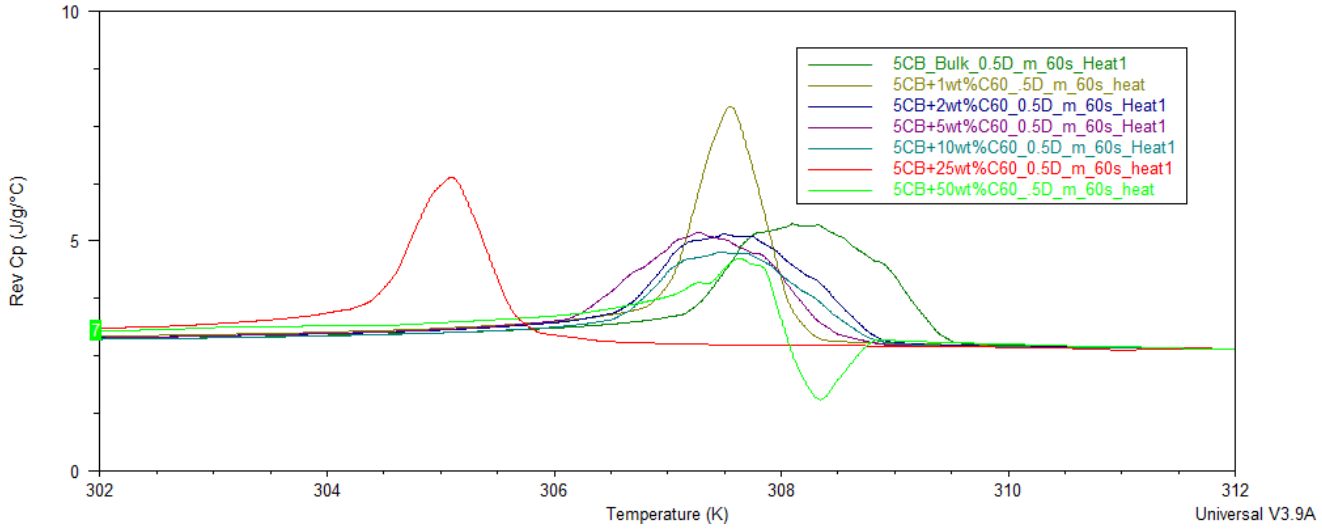

Figure 70 Reversible Cp 60s Modulation (heat)

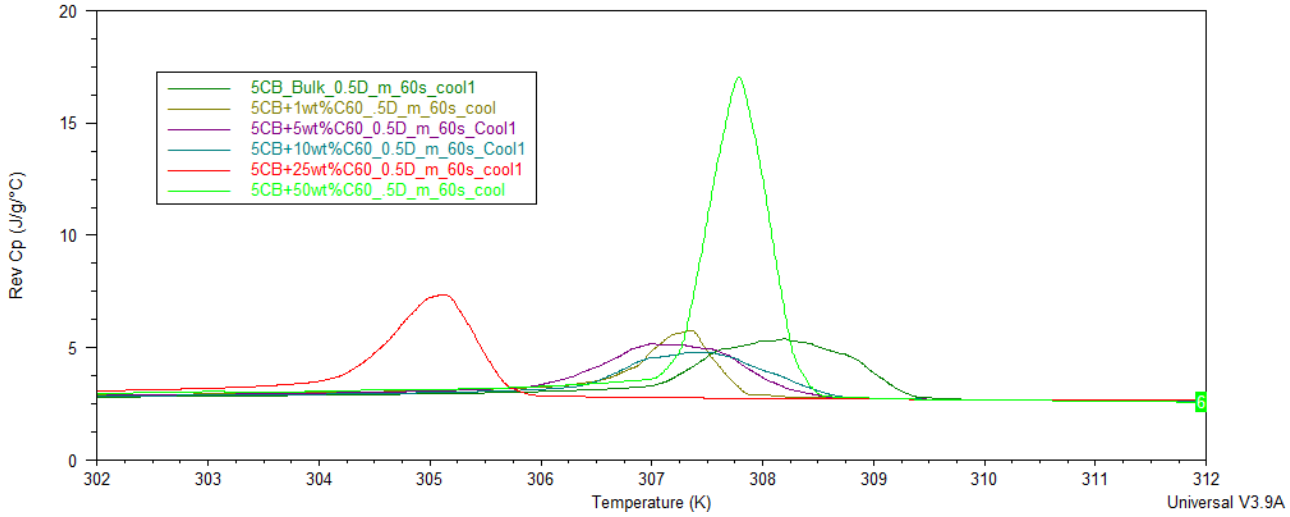

Figure 71 Reversible Cp 60s Modulation (cool)

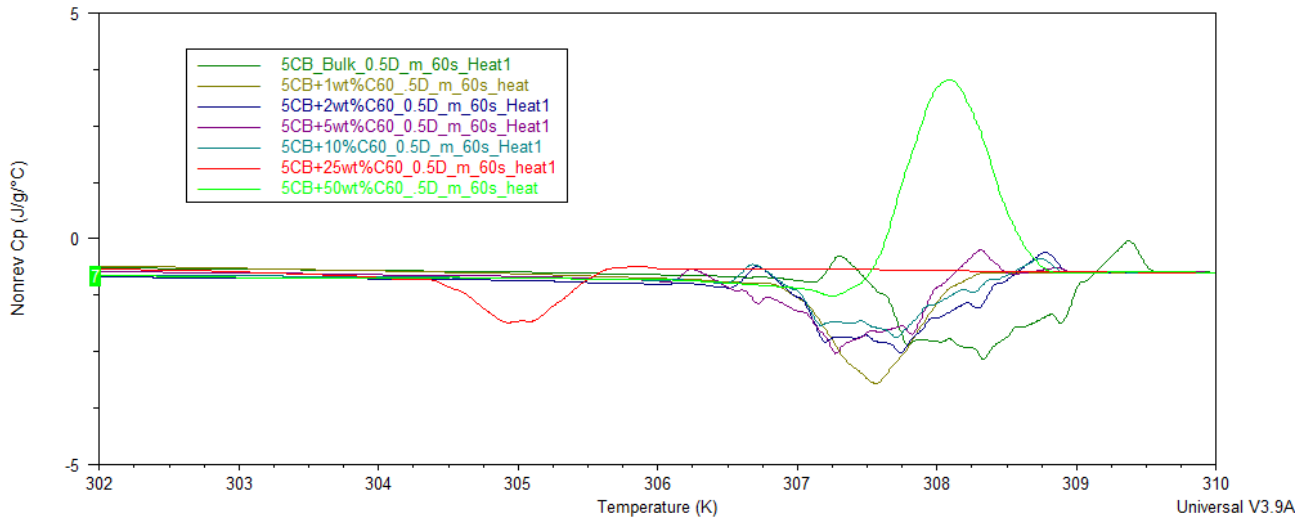

Figure 72 Nonreversible Cp 60s Modulation (heat)

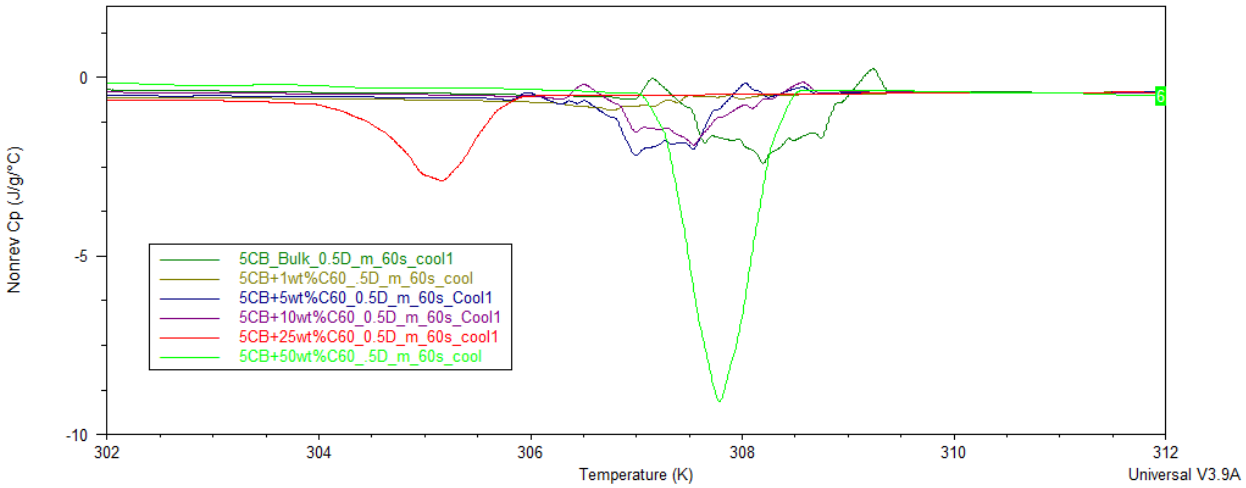

Figure 73 Nonreversible Cp 60s Modulation (cool)

75s Temperature Modulation

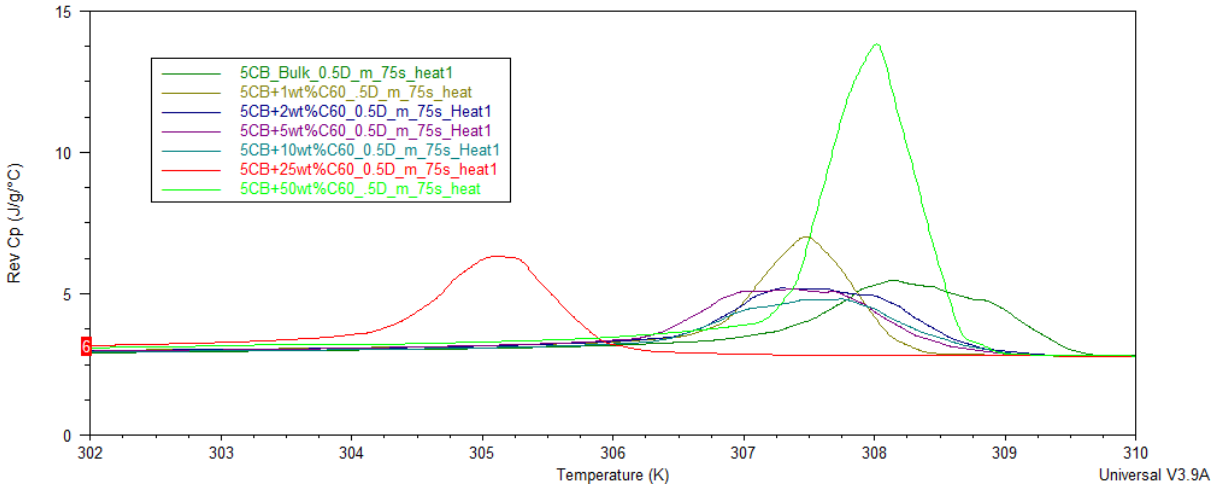

Figure 74 Reversible Cp 75s Modulation (heat)

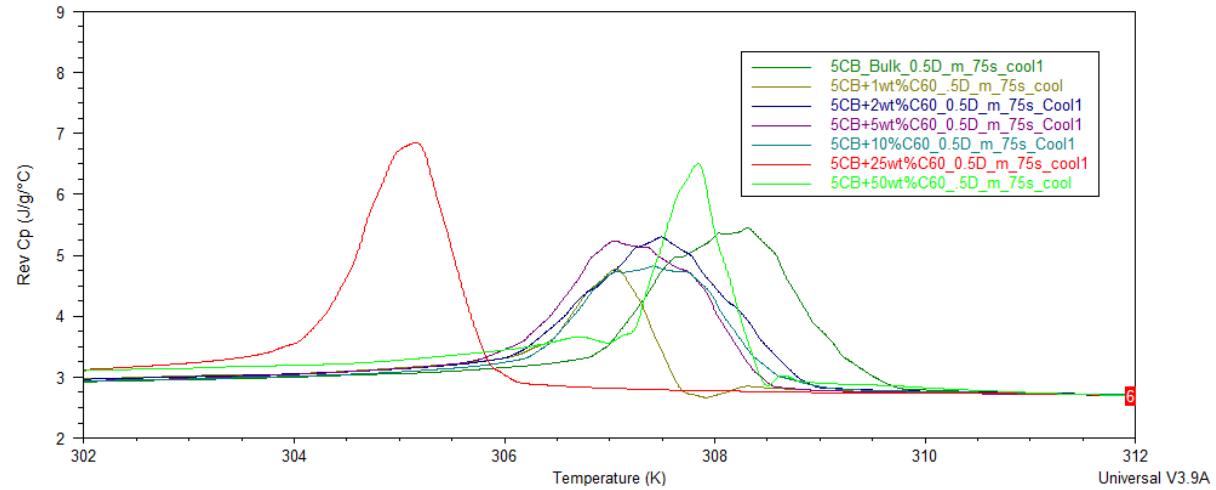

Figure 75 Reversible Cp 75s Modulation (cool)

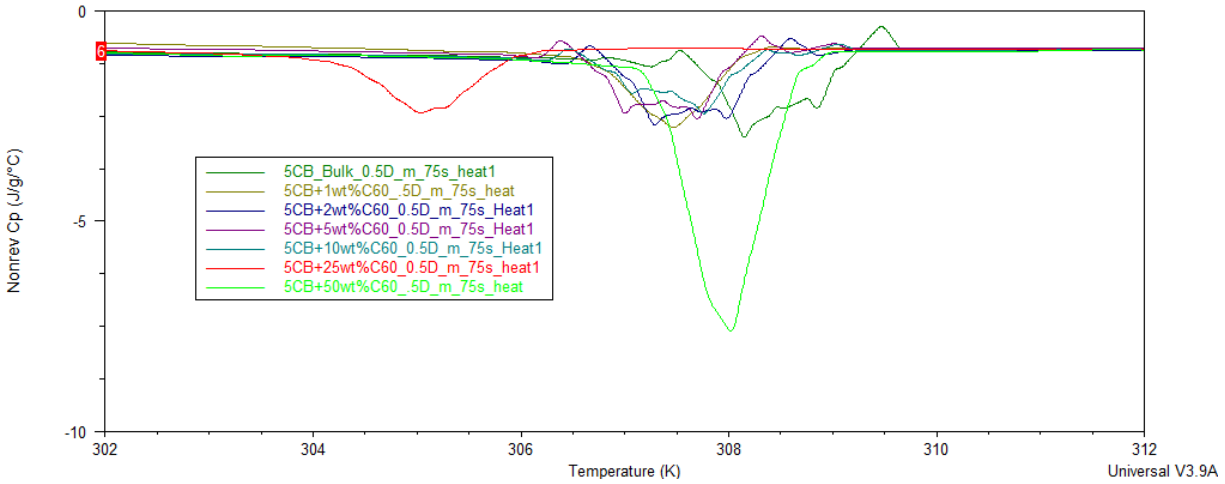

Figure 76 Nonreversible Cp 75s Modulation (heat)

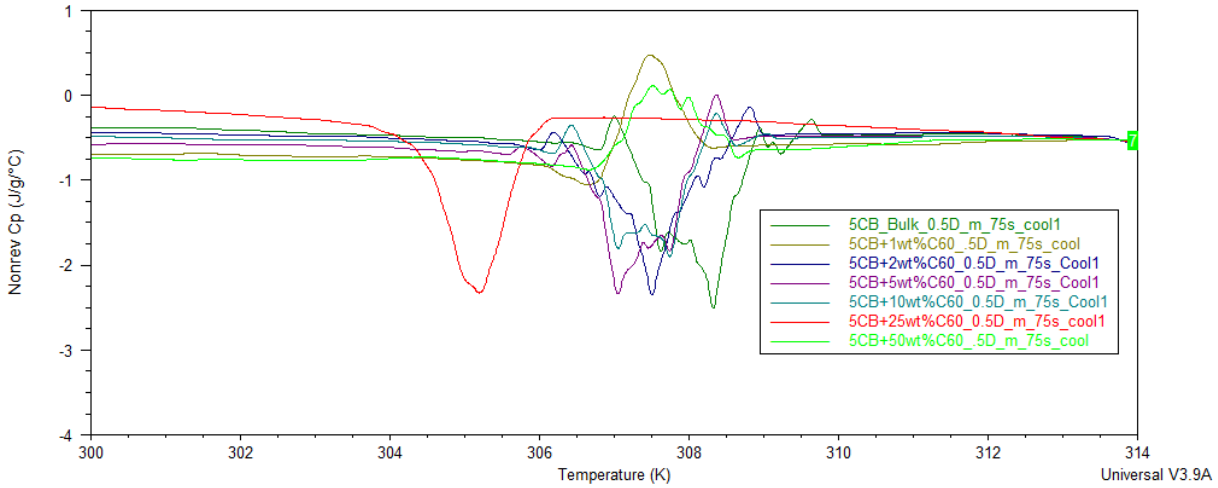

Figure 77 Nonreversible Cp 75s Modulation (cool)

100s Temperature Modulation

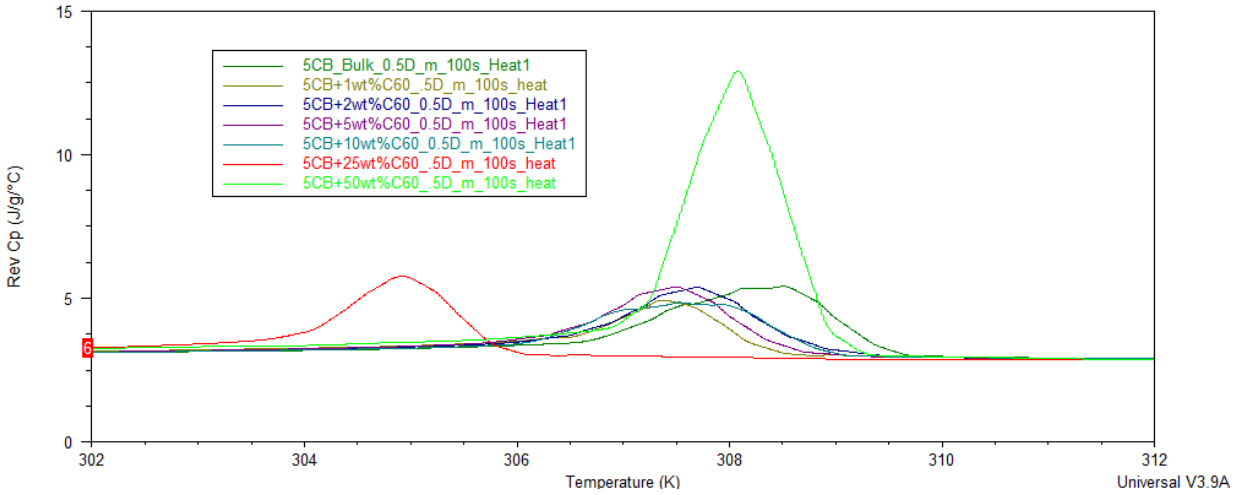

Figure 78 Reversible Cp 100s Modulation (heat)

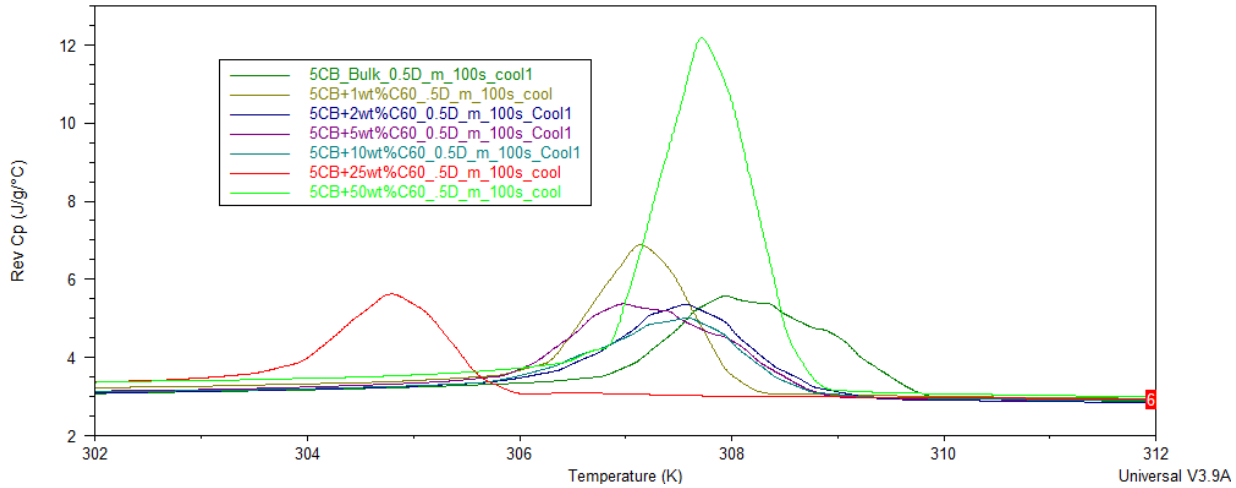

Figure 79 Reversible Cp 100s Modulation (cool)

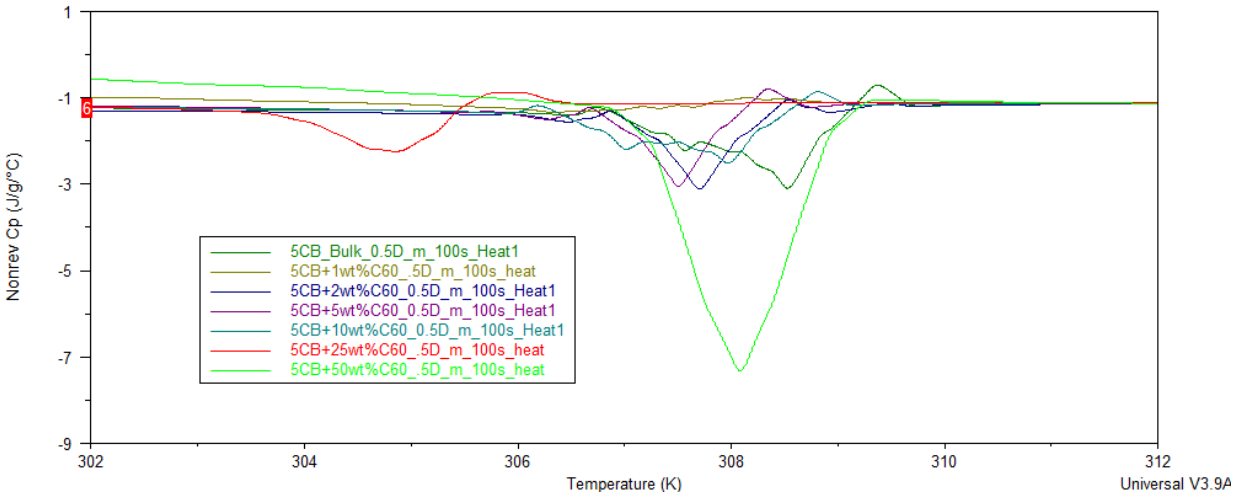

Figure 80 Nonreversible Cp 100s Modulation (heat)

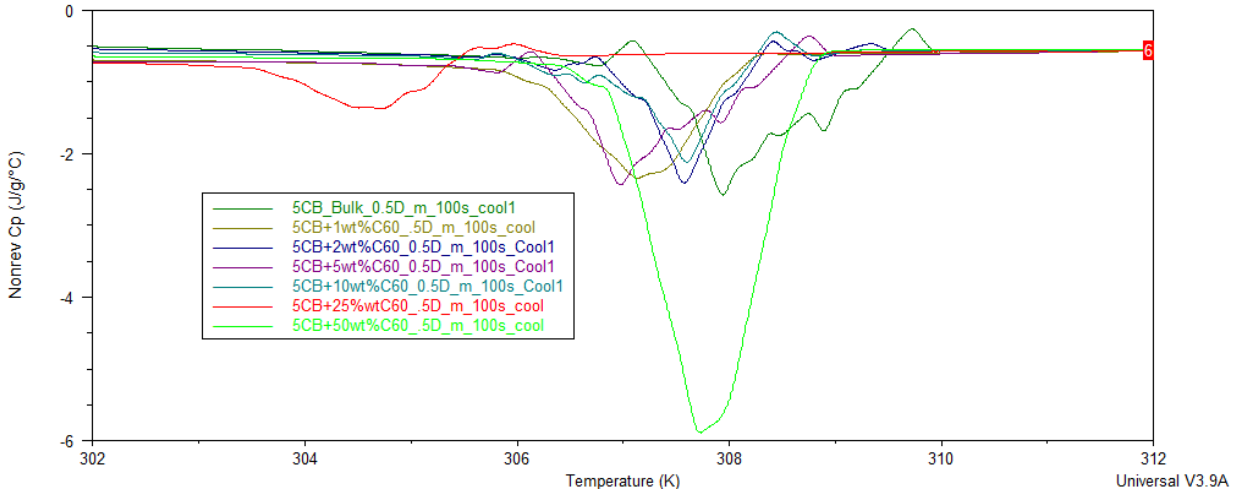

Figure 81 Nonreversible Cp 100s Modulation (cool)

C. Peak Temperature (K)

Scan Rate	.5 K/min		1 K/min		2 K/min		3 K/min		Averages	
	Heat	Cool	Heat	Cool	Heat	Cool	Heat	Cool	Heat	Cool
Bulk 5CB	308.17	308.21	308.43	308.02	308.8	308.23	308.49	307.79	308.47	308.06
1% wt. C60	307.52	307.01	307.45	307.3	307.79	307.24	307.85	307.55	307.65	307.28
2% wt. C60	307.51	307.44	307.59	307.47	308.17	307.27	307.48	307.29	307.69	307.37
5% wt. C60	307.4	307.18	307.5	307.27	307.51	307.33	307.31	307.2	307.43	307.25
10% wt. C60	307.51	307.44	307.69	307.25	307.4	307.03	307.66	307.39	307.57	307.28
15% wt. C60	307.42	307.19	307.49	307.25	307.46	307.26	307.44	306.96	307.45	307.17
20% wt. C60	307.8	307.45	307.77	307.01	307.88	307.56	308.14	306.53	307.90	307.14
25% wt. C60	304.89	304.9	305.17	304.9	305.35	304.9	304.86	304.75	305.07	304.86
50% wt. C60	308.21	307.74	308.01	307.68	308.02	307.6	307.99	307.7	308.06	307.68

Figure 82 Scan Rate Peak Temperature Comparison (heat&cool)

Modulation Period	30s		45s		60s		75s		100s		Averages	
	Heat	Cool	Heat	Cool	Heat	Cool	Heat	Cool	Heat	Cool	Heat	Cool
Bulk 5CB	308.17	308.21	308.17	308.25	308.1	308.21	308.13	308.3	308.39	308.08	308.19	308.21
1% wt. C60	307.52	307.01	307.48	307.22	307.52	307.35	307.44	307.09	307.44	307.14	307.48	307.16
2% wt. C60	307.51	307.44	307.54	307.44	307.51	N/A	307.29	307.52	307.69	307.61	307.51	307.50
5% wt. C60	307.4	307.18	307.25	307.22	307.29	307.05	307.36	307.05	307.47	306.96	307.35	307.09
10% wt. C60	307.51	307.44	307.47	307.31	307.47	307.52	307.47	307.44	307.54	307.57	307.49	307.46
25% wt. C60	304.89	304.9	304.97	305.08	305.08	305.11	305.12	305.16	304.9	304.78	304.99	305.01
50% wt. C60	308.21	307.74	308.04	307.89	307.65	307.78	308.04	307.82	308.08	307.74	308.00	307.79

Figure 83 Frequency Peak Temperature Comparison (heat&cool)

D. Enthalpy (J/g)

Scan Rate	.5 K/min		1 K/min		2 K/min		3 K/min		Averages	
	Heat	Cool	Heat	Cool	Heat	Cool	Heat	Cool	Heat	Cool
Bulk 5CB	4.32	4.318	4.353	4.379	6.587	6.912	2.014	1.337	4.3185	4.2365
1% wt. C60	3.175	2.069	2.985	3.008	5.188	3.874	4.467	0.7054	3.95375	2.4141
2% wt. C60	3.935	3.922	4.048	4.005	3.984	4.113	3.779	5.208	3.9365	4.312
5% wt. C60	3.874	3.802	3.863	3.862	4	3.982	3.287	3.365	3.756	3.75275
10% wt. C60	2.786	2.906	2.969	3	2.728	2.918	2.892	2.555	2.84375	2.84475
15% wt. C60	3.712	3.012	5.717	3.815	5.539	1.48	3.839	7.087	4.70175	3.8485
20% wt. C60	4.605	3.251	2.642	1.578	5.552	2.611	7.03	1.572	4.95725	2.253
25% wt. C60	3.872	3.859	3.98	3.324	3.799	2.711	2.644	5.971	3.57375	3.96625
50% wt. C60	4.468	6.235	4.227	8.737	5.374	11.46	9.439	9.673	5.877	9.02625

Figure 84 Scan Rate Enthalpy Comparison (heat&cool)

Modulation Period	30s		45s		60s		75s		100s		Averages	
	Heat	Cool	Heat	Cool	Heat	Cool	Heat	Cool	Heat	Cool	Heat	Cool
Bulk 5CB	4.32	4.318	4.708	4.692	4.972	4.99	4.651	4.722	4.781	5.126	4.6864	4.7696
1% wt. C60	3.175	2.069	4.325	4.289	4.801	3.259	4.14	2.333	3.13	4.884	3.9142	3.3668
2% wt. C60	3.935	3.922	4.348	4.367	4.459	N/A	4.514	4.535	4.348	4.382	4.3208	4.3015
5% wt. C60	3.874	3.802	4.203	4.169	4.294	4.3	4.483	4.45	4.191	4.756	4.209	4.2954
10% wt. C60	2.786	2.906	3.437	3.467	3.648	3.676	3.767	3.813	4.037	3.793	3.535	3.531
25% wt. C60	3.872	3.859	4.236	4.042	4.041	5.126	4.704	5.109	4.01	3.757	4.1726	4.3786
50% wt. C60	4.468	6.235	8.592	4.403	2.141	10.37	10.38	3.946	11.85	10.54	7.4862	7.0988

Figure 85 Frequency Enthalpy Comparison (heat&cool)

E. Full Width at half max (K)

Scan Rate	.5 K/min		1 K/min		2 K/min		3 K/min		Averages	
	Heat	Cool	Heat	Cool	Heat	Cool	Heat	Cool	Heat	Cool
Bulk 5CB	1.45	1.41	1.52	1.4	1.19	1.19	1.84	1.7	1.5	1.425
1% wt. C60	0.53	0.45	0.87	0.69	1.29	1.24	1.93	1.67	1.155	1.0125
2% wt. C60	1.38	1.42	1.49	1.38	1.47	1.57	2.31	2.22	1.6675	1.6
5% wt. C60	1.38	1.42	1.49	1.38	1.47	1.57	2.31	2.22	1.6625	1.6475
10% wt. C60	1.25	1.3	1.35	1.29	1.81	1.57	2.16	2.23	1.6425	1.5975
15% wt. C60	0.32	0.31	0.62	0.61	1.26	1.15	1.94	1.81	1.035	0.97
20% wt. C60	0.28	0.3	0.58	1.34	1.25	1.22	1.85	3.63	0.99	1.6225
25% wt. C60	1.55	1.58	0.98	0.76	1.39	1.52	1.9	1.9	1.455	1.44
50% wt. C60	0.34	0.37	0.63	0.6	1.27	1.19	1.85	1.8	1.0225	0.99

Figure 86 Scan Rate Full Width At Half Max Comparison (heat&cool)

Modulation Period	30s		45s		60s		75s		100s		Averages	
	Heat	Cool	Heat	Cool	Heat	Cool	Heat	Cool	Heat	Cool	Heat	Cool
Bulk 5CB	1.45	1.41	1.5	1.47	1.63	1.62	1.53	1.58	1.78	1.83	1.578	1.582
1% wt. C60	0.53	0.45	0.51	0.48	0.68	0.7	0.84	0.84	1.18	1.08	0.748	0.71
2% wt. C60	1.36	1.4	1.49	1.53	1.59	N/A	1.58	1.63	1.4	1.44	1.484	1.5
5% wt. C60	1.38	1.42	1.52	1.5	1.53	1.49	1.59	1.57	1.35	1.83	1.474	1.562
10% wt. C60	1.25	1.3	1.4	1.43	1.51	1.52	1.58	1.59	1.91	1.62	1.53	1.492
25% wt. C60	1.55	1.58	1.65	0.83	0.77	0.87	1.02	0.97	1.15	1.18	1.228	1.086
50% wt. C60	0.34	0.37	0.47	0.44	0.99	0.61	0.77	0.71	1.03	1.02	0.72	0.63

Figure 87 Frequency Full Width At Half Max Comparison (heat&cool)